Annu. Rev. Pharmacology and Toxicology. 1992. 32:623–69

DETERMINANTS OF METABOLITE DISPOSITION

K. Sandy Pang[1,2], Xin Xu[1,3], and Marie V. St-Pierre[1,4]

[1]Faculty of Pharmacy, University of Toronto, Toronto, Ontario, Canada
[2]Department of Pharmacology, Faculty of Medicine, University of Toronto, Toronto, Ontario, Canada
[3]Current Address: Merck Sharp and Dohme Research Laboratories, West Point, Pennsylvania 19486
[4]Current Address: Department of Physiology, School of Medicine, Tufts University, Boston, Massachusetts 02111

KEY WORDS: liver, intestine and kidney metabolism and excretion; drug and metabolite (primary, secondary, tertiary) extraction ratios; clearances (intrinsic, transmembrane, hepatic, renal, unbound); physiological variables (organ blood flow, protein binding, enzymic heterogeneity); metabolite sequential metabolism

INTRODUCTION

Much work in drug metabolism lends itself to in vitro and in vivo correlations, with the ultimate aim of applying data obtained from a much simplified in vitro system to predict events in vivo (1–4). Investigators have long recognized that the rates of metabolite formation in vitro, whether examined in a reconstituted system of purified enzyme,
tion, or intact isolated cells, are governed by the kinetic constants V_{max} and K_m for the underlying enzymes involved, and by the availability of the substrate or cosubstrate. However, the incubation conditions usually include high substrate and cosubstrate concentrations such that the enzyme becomes rate-limiting in the overall reaction.

Within the intact liver, enzymatic activities are parceled and localized zonally in discrete regions or cells; other potential rate-determining factors also exist. A substrate entering via the blood flow to the organ must gain access to the inside of the cell through the cell membrane, a first potential barrier, before it can utilize the metabolic/excretory systems within cells. Hence additional variables, namely blood flow (5, 6), the extent of drug binding to blood and tissue proteins (7–11), the permeation of molecules across biological membranes, and the structure of the organ need to be considered for the metabolism of drugs (for reviews, see refs. 12–15). In some instances, the rate of synthesis of a cosubstrate lags behind its rate of depletion; the cosubstrate will become rate-limiting under this circumstance (16, 17). For these reasons, observations in vitro often deviate from the results obtained in vivo. In vitro data often provide the metabolic profiling and not necessarily the quantitative formation of the metabolites within the intact organ.

For the whole body, multiple eliminating organs exist for drug biotransformation and excretion. A metabolite formed within an organ is likely to undergo immediate metabolism and/or excretion prior to leaving that organ. This fundamental observation: primary, secondary and tertiary metabolite formation and/or excretion arising from a single-pass delivery of a drug through the organ, has been expressed as the sequential first-pass effects of formed metabolites (18, 19); then all metabolites that are not excreted are poured into the venous output into the circulation. These metabolites also return to the elimination organs and are subjected to further metabolism; if polar, they will ultimately be excreted into either bile or urine. Thus, any given metabolite formed from the liver or other metabolizing organs may be sequentially metabolized/excreted either at its genesis or upon recirculation. The presence of multiple organs for formation of the given metabolite, and the anatomical arrangement of these metabolite formation organs are important considerations for metabolite disposition (20–23). Moreover, the occurrence of competing, eliminating organs for excretion and metabolism to other metabolites are additional factors for drug metabolism and metabolite disposition in vivo. For these reasons, in vitro findings often do not directly correlate with in vivo findings.

This review aims to update the various effects of the biochemical and physiologic determinants on metabolite disposition in the liver, the most important drug-metabolizing organ, and to describe the interorgan relationships between the liver and other drug-metabolizing organs for metabolite formation and removal. We emphasize structural aspects of the liver and the determinants of hepatic clearances of drug and metabolite. Drug elimination (metabolism and excretion) within the liver is discussed as a whole and in conjunction with the kidney, another metabolite formation and excretion

organ; these two organs pose as two parallel organs. We further discuss the liver and intestine, two serially arranged organs, and their contributions to the first-pass effect.

To date, most experimental and theoretical work has focussed on drug disposition. However, interest in the kinetics of metabolites is increasing because of their role in biological activity and toxicity. Existing treatments, including those presented in textbooks (24, 25), tend to be overly simplistic in approach and often fail to consider the sequential first-pass effect of the nascently formed metabolites, even though it has been shown experimentally that immediate sequential metabolism and/or excretion of nascently formed, primary metabolites occurs within a metabolite-formation organ, which subsequently reduces primary metabolite outflow concentrations (18, 19) and yields higher than expected concentrations of the secondary and tertiary metabolites (26). This observation is usually overlooked in considering primary, secondary, and tertiary metabolites formation. This aspect of immediate sequential metabolism is especially important in estimating total metabolite formation (oral vs intravenous administration (27)) for extensive or complex schemes of drug conversion to primary, secondary, and then tertiary metabolites. Numerous examples of extensive metabolic schemes exist, namely in the metabolism of diazepam to nordiazepam and temazepam, both of which form oxazepam then the oxazepam glucuronides (28), lidocaine to 3-hydroxylidocaine or MEGX, to 3-hydroxy MEGX or GX, then to the conjugated species or ring-opened metabolite (29, 30), other extensively metabolized compounds such as propranolol (31), and cyclophosphamide (32), where the terminal metabolite is the tertiary or quaternary species. These metabolic schemes usually entail competing pathways, which, to varying degrees, modulate the sequential metabolism of the species of interest.

DETERMINANTS OF METABOLITE KINETICS FOR LIVER

Structure of the Liver

The liver is the most important drug-eliminating organ in the body, and is capable of both metabolic transformation and biliary excretion. The liver is a highly specialized and heterogeneous organ (33–39), and its structure and attendant heterogeneities must be considered for a more quantitative expression of drug metabolism (metabolite formation) and subsequent metabolism of the metabolite. The smallest functional unit of the liver is known as the acinus (36–38), which consists of a terminal portal venule and hepatic arteriole, a bile duct, lymph vessels, and nerves. A zonal relationship exists between the cells constituting the acinus and the blood supply. The hepatocytes situated close to the portal space are first supplied with fresh blood (rich

in oxygen and nutrients), and zonation is contingent upon the oxygen tension at that locale. With a steady input of oxygen entering the organ, a concentration profile in space is created, declining from inlet to outlet. Zone 1 (or periportal region) is closest to the entry of the hepatic artery and portal vein or the portal triad and is of the highest oxygen tension. Zone 3 (perihepatic venous or pericentral region) is near the exit, where oxygen tension is lowest. An overlapping zone 2 (or midzonal) region exists, where the oxygen tension is intermediate. However, the shape of the profiles can be altered as zone 2 cells can be recruited to behave more like zone 1 or 3 cells, depending on flow and oxygen utilization. These different acinar regions are specialized in mediating various biochemical/physiologic processes (40–43; for review, see ref. 44).

The sinusoids are surrounded by single plates of hepatocytes of similar lengths and lined by endothelial cells containing sieve plates with open fenestrae. There is also a freely accessible Disse space (a functional extracellular interstitial space that allows for equilibrative exchange). The velocities of blood elements flowing through the various sinusoids differ and are displayed as skewed outflow profiles (or dispersion of elements) upon injection of noneliminated reference indicators (for example, labeled red cell, albumin, sucrose, or water) (5, 45). Functional metabolic (44) and excretory (46, 47) heterogeneities are known to exist, as cells in different zones of the liver are distinct, both morphologically and functionally. Discrete carrier-mediated systems present for amino acid or carbohydrate transport have recently been found (41, 43).

Biochemical and Physiological Determinants of Drug and Metabolite Processing

The physiologic and biochemical factors governing drug and metabolite clearances have been extensively reviewed (48–59). Several mathematical descriptions have evolved to describe the interrelationship of membrane permeability, binding to red blood cells and plasma and tissue proteins, enzymatic activity, cosubstrate availability, and organ blood flow on the uptake of drugs and metabolites. A recent review compared the properties and steady-state mathematical relations of several hepatic clearance models ("well-stirred", "parallel tube", "dispersion", and "enzyme-distributed") for their ability to predict metabolite formation and elimination (59). Only the enzyme-distributed model, which best describes metabolite formation and elimination, is covered in detail here.

First, for the intact organ, the steady-state rate of loss of drug, v_{ss}, is solely attributed to the rate of elimination (metabolism and excretion) inasmuch as tissue binding is completed and will not contribute to the rate of loss. According to Fick's principle, this is given by:

$$v_{ss} = Q(C_{In} - C_{Out}) \quad 1.$$

where Q is the hepatic blood flow rate, and C_{In} and C_{Out}, respectively, denote the steady-state blood input and output drug concentrations. The rate of removal, when expressed in terms of the rate of drug presentation, QC_{In}, gives the steady-state hepatic extraction ratio, E_{ss}

$$E_{ss} = \frac{Q(C_{In} - C_{Out})}{QC_{In}} = \frac{(C_{In} - C_{Out})}{C_{In}} \quad 2.$$

The total rate of loss is the summation of the saturable metabolic and excretory processes occurring, and is

$$v_{ss} = \sum_{i=1}^{n} \frac{V_{max_i} C_{L,u}}{K_{m_i} + C_{L,u}} = \sum_{i=1}^{n} CL_{int_i} C_{L,u} \quad 3.$$

where V_{max_i} and K_{m_i} denote the maximum velocity and the Michaelis-Menten constant, respectively, for the ith saturable eliminatory pathway; CL_{int_i}, or $[V_{max_i}/(K_{m_i} + C_{L,u})]$, is the intrinsic clearance, the volume of hepatocellular water space cleared of drug per unit time for the ith pathway. The ratio dwindles to a constant, V_{max_i}/K_{m_i}, under first-order conditions at $K_{m_i} >> C_{L,u}$, the unbound substrate concentration in liver. For a primary metabolite (mi) that is not further metabolized, its steady-state rate of formation v_{ss}^{mi} is given by the sum of the steady-state efflux rate and the biliary excretion rate when the single-pass perfused liver is used:

$$v_{ss}^{mi} = QC_{Out}(mi) + \frac{\Delta A_e(mi)}{\Delta t} \quad 4.$$

For a primary metabolite (mi) that is further metabolized, the steady-state rate of formation (v_{ss}^{mi}) is given by the sum of the efflux rates of mi and all metabolites arising from mi in hepatic venous blood and in bile. The apparent fractional removal of the formed primary (or secondary) metabolite can be expressed as the apparent extraction ratio of the primary or secondary metabolite, and is the ratio of the elimination rate of formed metabolite to the formation rate of metabolite.

Distributed-in-Space Processing of Drug and Metabolite

When a substrate is taken up and irreversibly eliminated, a concentration profile in space is created during the steady state, declining from inlet to outlet (60–63). This concentration profile of substrate in space (with its corresponding input-output concentration difference), is related to, and must be accounted for by the underlying hepatic microcirculatory structure and physiologic and biochemical processes. The metabolic zonation within the liver (64–86) has been known to influence drug and metabolite processing within the liver. Uptake of substrate by successive cells along the direction of flow, from the inlet to the outlet of the liver, could be viewed as a distributed-in-space phenomenon. The events are dependent on substrate influx for recruitment of metabolic/ excretory activities, and efflux, in a fashion linked to the delivery by flow (12, 14, 56, 86); the influx, elimination, and efflux characteristics are modulated by substrate binding to blood (red blood cells (87–89) and plasma proteins (9, 90–98)), the perfusing medium, and to tissue (7, 8, 10, 11); the general dogma is that the free substrate is the species that is transported across membranes and becomes eliminated (90–94, 97). Similar consideration must then be given to metabolites formed within hepatocytes; after formation, each metabolite is either potentially subjected to immediate additional metabolic and/or excretory events, or reenters the sinusoid and is then exposed to the interactions with hepatocytes downstream from its site of formation before it finally leaves the liver (12, 55, 76–78, 86). For this reason, a metabolite formed within the liver is expected to undergo different extents of metabolism/excretion, including the predominant formation of various metabolites, than a metabolite (preformed) entering the liver from the circulation (18, 99–103). This disparity is due to different points of metabolite introduction in the organ, even though the same transport and elimination mechanisms are involved in subsequent processing. The whole must thus be viewed within the context of the microcirculatory events and the functional heterogeneities in the liver.

Enzyme Zonation

Zonal enzymic distribution is one of the most important determinants in metabolite formation and immediate sequential metabolism of the nascently formed metabolite within the liver. Metabolic zonation within the liver lobule has been well studied during the past few years. Direct and indirect techniques have shown an enriched presence of the cytochrome P-450s, epoxide hydrolase, glutathione-S-transfersases, carboxylesterases (64–66, 69, 80, 85, 104) and UDP-glucuronosyltransferases in the perihepatic venous region (Zone 3) (67, 68, 71, 72) [glucuronidation activity is also found to be evenly distributed in zones 1, 2, and 3 (73, 76–78)], with the sulfotransferases predominating in the periportal region of the liver (74–79) (Table 1). Elimination of a

Table 1 Relative enzymic activities found by immunohistochemical and staining techniques, microdissection, and by prograde and retrograde perfusions and HAPV and HAHV perfusion of the rat liver

Noted Metabolic Heterogeneities				
Anterior	Even	Posterior	Drug Examples	References
		Mixed-function oxidases cytochrome P-450		64, 65
		NADPH cytochrome P-450 c Reductase		66
		UDP-glucuronosyltransferase	7-Hydroxycoumarin	67, 68, 71, 72
		Epoxide Hydrolase		70
		Glutathione-s-transferase		69
	Alcohol dehydrogenase			83
	Arylsulfatase β-glucuronidase			81, 82
Sulfation			Acetaminophen N-OH-2-acetylaminofluorene	79, 80 74, 75
		O-Deethylation	Phenacetin	79, 80
		Carboxylesterase	Enalapril	85, 104
Sulfation		Glucuronidation	7-Hydroxycoumarin	71, 72
Sulfation	Glucuronidation	Hydroxylation	Salicylamide	78
	Hydroxylation	N-Deethylation	Lidocaine	84

substrate/metabolite occurs only when it is present along the sinusoid and if it gains access into hepatocytes. Given the marked enzyme heterogeneities noted for Phase I and Phase II reactions, the nature and proportion of conjugates formed as primary or secondary metabolites arising from parallel or sequential pathways is expected to differ (103).

The roles of enzyme zonation on competitive and sequential drug metabolism have been illustrated both theoretically and experimentally. Conceptually, an enzymic distribution describes the density of the enzyme or $V_{max,x}$ along the length of the sinusoid, L; two such enzymic systems are depicted schematically in Figure 1. The relative locations of each of these two systems may be described with respect to its median (or center) of enzymic distribution, the plane that divides total enzymatic activity (total V_{max} or $\int_0^L V_{max,x}dx$) into halves. The median or the "median distance" serves to interrelate the distance between inlet of the liver and the bulk of the enzyme. System I is viewed as an anterior pathway in relation to System II, since its median (or center) of distribution precedes that for System II. These two systems (I and II) may represent competitive pathways or sequential pathways.

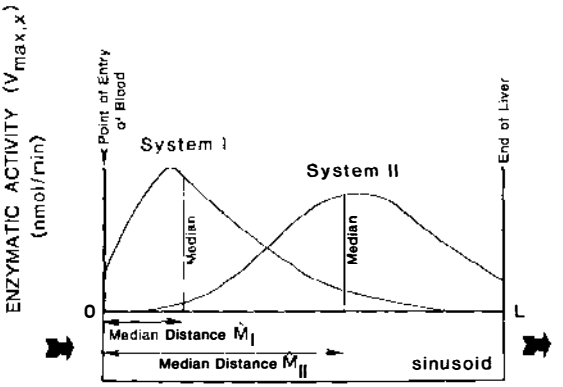

Figure 1 The distributed-in-space phenomenon in drug processing. A schematic representation of uneven distribution of drug metabolizing enzymes in the liver, Systems I and II, which are either involved in parallel, competing, or sequential metabolic pathways. Drug processing occurs along the direction of flow of substrate, from left to right, in a distributed-in-space fashion. The enzymic distributions of Systems I and II are described by the median distances, the distance from the inlet of the liver to the median (plane that divides the amount of enzyme into equal halves). As shown, System I is anteriorly localized relative to System II along the direction of flow of substrate.

PARALLEL PATHWAYS Conjugation by sulfation and glucuronidation of most phenolic substrates is the simplest example of parallel, metabolic pathways. Sulfation is often a higher-affinity, lower-capacity pathway in relation to glucuronidation. A substrate coming into contact with hepatocytes along the direction of flow first accesses the anteriorly located enzyme system (System I, sulfotransferases) to generate the corresponding sulfate conjugate; glucuronidation by System II, the posteriorly located competitive system, occurs only when residual substrate arrives downstream for recruitment of such activities. Hence the concentration of substrate at x is related to its removal at points preceding x and at x.

For highly extracted compounds, where outflow concentrations are much lower than the corresponding input concentrations, a steep intrahepatic gradient exists during the steady-state flow of substrate into the liver; the converse is true for poorly extracted compounds. Anterior pathways affect the formation of metabolites downstream in highly extracted compounds the greatest; this occurs at low concentration wherein not all downstream hepatocytes are metabolically recruited because of depletion of substrate due to upstream metabolism. At intermediate concentrations that are saturating for the anteriorly located sulfation system, a proportionally higher substrate flux reaches the downstream region to effect glucuronidation, rendering disproportionately higher glucuronidation rates; at higher concentration ($>> K_m$s), all enzymic systems (anterior and posterior) will be recruited by the substrate, and the role of enzymic heterogeneity in metabolite formation becomes attenuated and unimportant (105, 106). Salicylamide, gentisamide, and harmol are highly cleared phenolic substrates that exhibit the typical compensatory rise in glucuronidation rate with concentration (102, 103, 107; Figure 2). With suppression of sulfation by a specific inhibitor, 2,6-dichloro-4-nitrophenol (DCNP), the aberrancy observed previously for glucuronidation of harmol and salicylamide disappears (103, 108); Michaelis-Menten like kinetics are now observed for glucuronidation (Figure 3).

SEQUENTIAL PATHWAYS Because metabolite formation must necessarily precede metabolite elimination, events such as drug uptake followed by biotransformation would affect further metabolism/excretion of the immediately formed metabolite, compared to that for a preformed metabolite which is entering as input to the organ and is independent of the kinetic behavior of drug. Theoretical examinations of the fates of primary (M_1), secondary (M_2) and tertiary (M_3) metabolites upon steady-state input of a precursor drug (P) or preformed metabolites into isolated hepatocytes and the intact liver revealed differences (59, 109, 110). For flow-limited precursor drugs and metabolites (that is, rapid entry of all species across liver cell

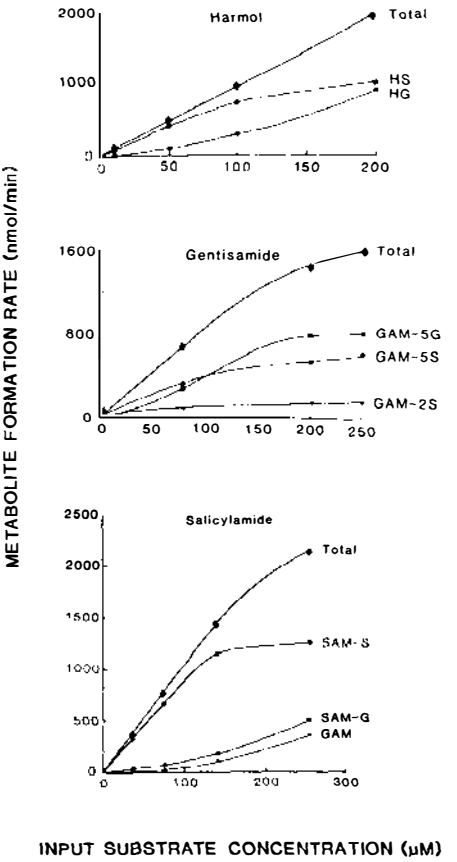

Figure 2 Concentration-dependent formation of metabolites of harmol, gentisamide, and salicylamide in the single-pass perfused rat liver preparation (data from ref. 102, 103, 107). Note the disproportionate increases for glucuronidation and hydroxylation rates with concentration.

membranes, no barrier-limitation), the apparent extraction ratios of the primary and secondary metabolites, $E(M_1,P)$ and $E(M_2,P)$, respectively, arising from drug (P) differ from the extraction ratios ($E(M_1)$ and $E(M_2)$) obtained with the administration of the preformed metabolite species M_1 and M_2, respectively. In both systems, a rank order is found: $E(M_1) > E(M_1,P)$ and $E(M_2) > E(M_2,M_1) > E(M_2,P)$, that is, the extraction ratio of a generated, lipophilic metabolite (M_1 or M_2) will be less than, and at best equal to, that after its administration into the organ as a preformed species. The discrepancy

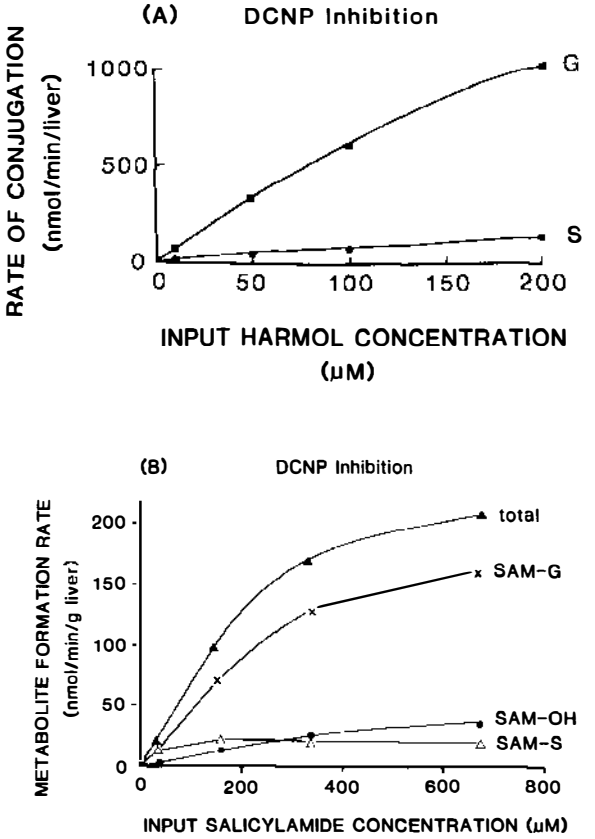

Figure 3 Suppression of sulfation rates of harmol (A) and salicylamide (B) with 2,6-dichloro-4-nitrophenol (DCNP). Note the disappearance of the non Michaelis-Menten-like behaviors for glucuronidation and hydroxylation observed in Figure 2 (data from ref. 103, 108).

is further augmented by an increasing number of steps involved in the formation of the metabolite (59). The degree to which these extents vary also depends on the distribution of enzymic systems for metabolite formation and metabolism, and the intrinsic clearances for the precursors. But the kinetic phenomenon appears to be less independent of the presence of competing pathways under first-order conditions (14, 59).

This situation in isolated hepatocytes is illustrated with several hypothetical, simulated examples that show the rank order (59, 110; Figure 4). The extent of sequential metabolism of a generated metabolite is maximal when associated with precursor compounds with high intrinsic clearances for formation relative to the intrinsic clearance for metabolism of the metabolite, and is

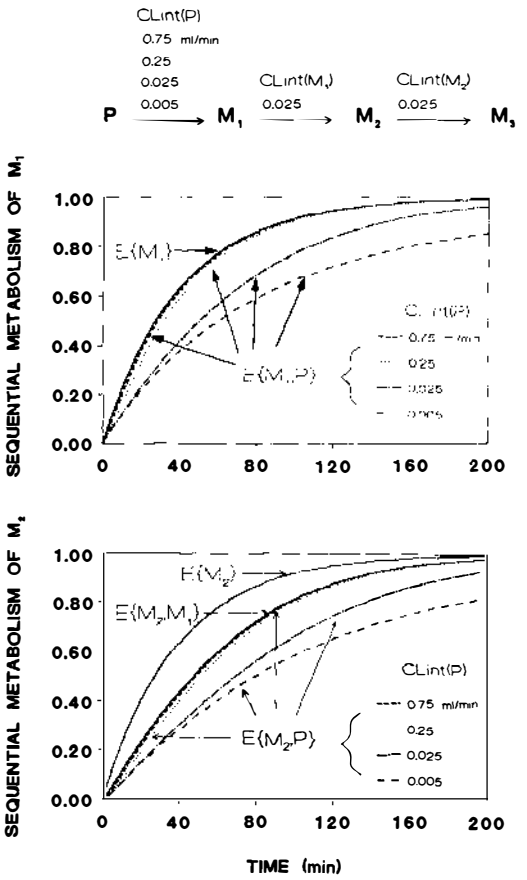

Figure 4 Simulated extents of sequential metabolism [drug (P) conversion to its primary (M_1), then secondary (M_2), and tertiary (M_3) metabolites] in a well-mixed system for a primary metabolite M_1 after administratin of P (expressed as $E\{M_1,P\}$) (A), and for a secondary metabolite M_2 after administration of P (expressed as $E\{M_2,P\}$), or M1 (expressed as $E\{M_2,M_1\}$) (B). Values of intrinsic clearances (ml/min) for the metabolism of P, M_1, and M_2 are shown. (See text for details.)

least for precursors with very small formation intrinsic clearances. Rapid formation of the primary (or secondary) metabolite furnishes that metabolite for avid metabolism and lessens the "lag" observed when its extent of sequential metabolism is compared to that found for the preformed primary (or secondary) metabolite. When formation of the metabolite is extremely rapid, the extents of metabolism of the preformed and generated primary metabolites become identical. If formation of metabolite is slow, however,

sequential metabolism lags behind that for preformed metabolite, and the rank order hence becomes apparent.

This kinetic phenomenon is displayed in the sequential processing of tracer [^{14}C]phenacetin to [^{14}C]acetaminophen and [^{14}C]acetaminophen sulfate conjugate and the metabolism of [^{3}H]acetaminophen to [^{3}H]acetaminophen sulfate conjugate in rat isolated hepatocytes (110). In this apparently, well-mixed pool of hepatocytes consisting of cells from zones 1, 2, and 3, preformed acetaminophen (labeled with tritium) readily enters hepatocytes to become sulfated. For the lipophilic precursor, phenacetin, the membrane barrier also appears to be absent in isolated hepatocytes such that both drug and metabolite gain ready access into cells. [^{14}C]Acetaminophen formed from [^{14}C]-phenacetin, however, yields proportionately less labeled sulfate than preformed [^{3}H]acetaminophen under first-order conditions (Figure 5).

A similar phenomenon is observed in the single-pass perfused rat liver preparation, where enzyme heterogeneity is present and formation followed by metabolism of the formed metabolite displays the kinetic phenomenon, now in a distributed-in-space fashion. In the intact liver, the [^{14}C]acet-

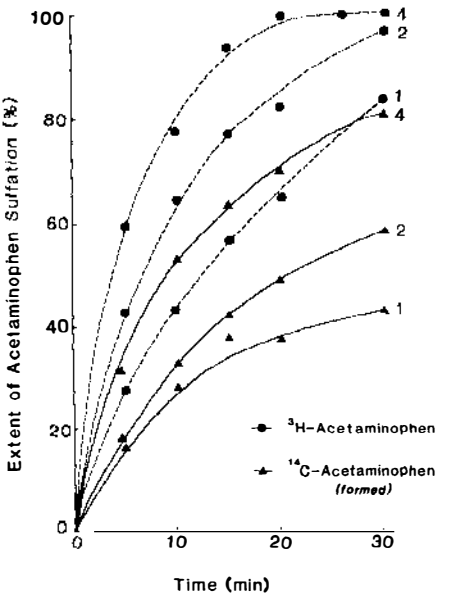

Figure 5 Reduced extents of sulfation for [^{14}C] acetaminophen generated from [^{14}C]phenacetin than for preformed [^{3}H]acetaminophen in isolated, rat hepatocytes. Incubation was performed in 5 ml, containing 4, 2, and 1 ml cell suspensions (numbers appearing on graph). (Data reproduced from ref. 110, with permission.)

aminophen formed from [^{14}C]phenacetin downstream (or perihepatic venous region) is unable to use sulfation activities within hepatocytes upstream (or periportal region) (79). The unfavorable enzyme stacking tends to steer towards a lesser extent of sequential sulfation of the formed [^{14}C]acetaminophen in relation to that after administration of preformed [^{3}H]acetaminophen to the liver. $E(M_1)$ for preformed [^{3}H]acetaminophen (0.72) is greater than $E(M_1,P)$ or 0.56 for [^{14}C]acetaminophen formed from [^{14}C]phenacetin. Even when all O-deethylase and sulfation activities were evenly distributed within the liver, $E(M_1)$ would persist in being greater than $E(M_1,P)$ because of the kinetic phenomenon.

Sequential metabolic processing has recently been examined in perfused mouse liver studies for the extensive metabolic conversion of diazepam (P) to lipophilic, intermediate metabolites, nordiazepam (M_1) and temazepam, both of which form oxazepam (M_2), then to terminal, diasteriomeric oxazepam glucuronides (M_3); temazepam formation from diazepam and as a contributor of oxazepam, M_2, is a very minor and negligible pathway (100, 101). The extraction ratios of the oxazepam precursors, diazepam ($E(P)=0.96$) and preformed nordiazepam ($E(M_1)=0.4$), are found to be high and intermediate, respectively (100, 101), whereas that for preformed oxazepam $E(M_2)$ is low (0.125) (99). The extraction ratio of formed nordiazepam, derived from diazepam [$E(M_1,P)$ or 0.427] compares well with that observed after the administration of preformed nordiazepam ($E(M_1)$ or 0.4). The comparison of the extraction ratios of oxazepam, derived from nordiazepam [$E(M_2,M_1)$ or 0.06] and diazepam [$E(M_2,P)$ or 0.069] reveals that these values are lower than that for preformed oxazepam (0.125). The similar $E(M_1,P)$ and $E(M_1)$ values for nordiazepam metabolism may be explained by the rapid, initial formation step from diazepam; this high intrinsic clearance first step further renders virtually identical values of $E(M_2,M_1)$ and $E(M_2,P)$ for oxazepam metabolism. However, because the second step, formation of oxazepam from nordiazepam, is comparatively slower, $E(M_2,M_1)$ and $E(M_2,P)$ are less than $E(M_2)$. If the formation of nordiazepam from a precursor is slower than that observed for diazepam, the sequential metabolism of nordiazepam to oxazepam then the oxazepam glucuronides is expected to lag behind that for preformed nordiazepam, and the following rank orders for the kinetic phenomenon, $E(M_1) > E(M_1,P)$ and $E(M_2) > E(M_1) > E(M_2,P)$, will readily become apparent.

SECONDARY METABOLITE FORMATION Salicylamide (SAM, 2-hydroxybenzamide) is competitively metabolized by the single-pass perfused rat liver primarily to its sulfate and glucuronide conjugates, and is hydroxylated at the 5-position only to a minor extent to form gentisamide (GAM). GAM is sulfated at both the 2- and 5-positions (GAM-2S and GAM-5S) and glucur-

onidated at the 5- (GAM-5G) position. When preformed genetisamide is given to the single-pass perfused rat liver, the sulfate conjugates are major metabolites and GAM-5G is a minor metabolite (102). However, when SAM is delivered to the single-pass perfused rat liver, the major sequential metabolite arising via GAM is GAM-5G, with GAM-2S and GAM-5S as virtually undetectable metabolites (103). The astoundingly different proportions of sequential metabolites, which arise through administration of SAM or GAM to the once-through rat liver preparation, is explained by a downstream SAM hydroxylation (for GAM formation), which is in close proximity to the glucuronidation system. When GAM enters the liver, by contrast, sulfation, which is the anterior pathway, will be initially recruited to yield sulfate conjugates as the major metabolites.

Liver Blood Flow

The role of hepatic blood flow on drug removal has been well studied (5, 6, 111–115), but is seldom extended to describe metabolite formation. When substrates are categorized as highly ($E_s \cong 1$), intermediately, or poorly ($E \cong 0$) extracted compounds, a systematic variation in behavior is found. A highly cleared compound is almost completely removed due to the underlying high liver metabolic/excretory activities, and hence the clearance of these compounds becomes rate-limited by organ blood flow rate; for poorly cleared compounds, clearance is restricted by the intrinsically poor removal ability of the organ for the substrate and not by sluggish delivery of substrate by flow (48–50, 56). For highly cleared compounds, E_{ss} is not readily perturbed by changes in flow; for poorly cleared compounds, a reduction in liver blood flow rate results in a longer transit time and an increase in extraction ratio, whereas with a faster flow rate, the opposite will be observed. Changes in organ blood flow on metabolite formation, however, affect parallel and sequential metabolic pathways differently (116–118).

PARALLEL PATHWAYS The manner in which two conjugative pathways compete in drug removal has been investigated both theoretically (105, 106, 117, 118) and experimentally (116, 117) in the single-pass perfused rat liver preparation at varying flow rates (8 to 16 ml/min). For evenly distributed conjugative systems, or for an anteriorly distributed sulfation and posteriorly distributed glucuronidation system, the changes in S (sulfation rate) are expected to parallel those for E_{ss} with flow, since drug processing (reflected by E_{ss}) is mostly conversion to the sulfate conjugate, due to its low K_m. The changes for G (glucuronidation rate), however, are different and will vary according to the drug input concentration. G, the less avid and posterior pathway, is apparently influenced by diametrically opposed factors induced by flow: substrate supply and sojourn time (118), and these two opposing

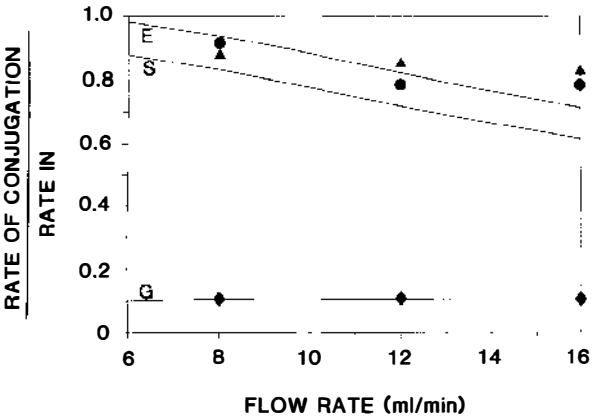

Figure 6 Influence of organ blood flow on the extraction ratio of harmol (10 uM) and formation of harmol sulfate and harmol glucuronide conjugates. The flow-induced changes of harmol sulfation (▲) parallel those for harmol extraction ratio (•). No apparent change is observed for harmol glucuronidation (♦) due to the counterbalancing effects of reduced sojourn time for drug and higher availability of drug downstream at increased flow rates (data from ref. 118, with permission).

effects are apparent at low input concentrations ($<< K_m$s), where substrate availability and not enzyme is rate-limiting. At low flows (6–8 ml/min), avid sulfation (high affinity pathway) occurs, sparing almost no substrate for glucuronidation (low affinity pathway). Hence, despite a longer sojourn of drug in the liver, little G will be observed as substrate is not available. At higher flow rates (14–16 ml/min), which furnish diminished drug transit times, more substrate is spared from sulfation for formation of the glucuronidc at a faster rate of drug transit. For these reasons, G will be seemingly unaltered upon flow changes from 6 to 16 ml/min at input concentrations $< K_m$s, when these two opposing effects cancel each other out. This pattern is displayed in harmol conjugation, where decreased (periportal) sulfation and an unchanged glucuronidation are observed with increasing flow (Figure 6).

SEQUENTIAL PATHWAYS For any preformed species, drug or preformed metabolite entering the liver, an inverse relationship between the extraction ratio and flow exists, regardless of enzymic distribution. The effect of flow on the apparent hepatic extraction ratio of the generated metabolite in sequential pathways is similar to that for the preformed metabolite (and its precursor), except for the persistently higher extent of metabolism for the preformed over the formed metabolite. This has been attributed to the longer sojourn time of a preformed species vs a generated species in flow-limited situations (drug and metabolite do not encounter hepatocyte membrane as a barrier) (6, 59, 109, 118). Pending the enzyme model for overlap of enzymes, the extent of

sequential metabolism of the generated metabolite differs; it is higher for a greater degree of overlap between the formation enzyme and the enzyme for sequential metabolism. The predictions match the observations for tracer [^{14}C]acetaminophen formed from [^{14}C]phenacetin (downstream) and for tracer preformed [^{3}H]acetaminophen sulfation (upstream) with flow changes in the single-pass rat liver preparation (118). The extents of metabolism of all species, [^{14}C]phenacetin, preformed [^{3}H]acetaminophen, and formed [^{14}C]acetaminophen, are decreased with increasing flow.

Protein Binding Effects

The influence of drug-protein binding on drug disposition has been both well recognized and intensively studied (9, 61, 90–98, 116–122). The generally accepted view is that pharmacological activity and the rate of removal within drug metabolizing/excretory organs are related to the unbound species. Hence changes in the unbound concentration in the body, expressed also as changes in the unbound fraction, may on occasion elicit toxic or subtherapeutic outcomes. This is especially true for highly bound compounds like warfarin, bilirubin, dicumarol, and valproic acid (123–125).

Because of the existence of a concentration gradient along the liver sinusoid due to irreversible drug loss, the outlet concentration is lower than the inlet. The lowered substrate/protein ratio at the outlet is expected to result in decreases of the unbound fraction; such a decrease is more apt to occur for highly bound drugs that are highly cleared since the concentration gradient along the sinusoid is the steepest (119, 126). The dynamics of substrate removal and the induced changes in the unbound fraction along the flow path at varying inlet concentrations, in the presence of heterogeneously distributed enzymic systems, have been examined in concert for substrate removal under varying input substrate concentrations (126).

Since protein binding is viewed in most instances as a reversible process and describable by the Langmuir isotherm, the unbound plasma concentration for a single class of N number of equivalent binding sites of identical affinity constant, K_A, can be solved analytically and described with respect to the total plasma concentration, C_P as follows (126):

$$C_{P,u} = \frac{-(1 + NK_A[P_t] - K_A C_P) + \{(1 + NK_A[P_t] - K_A C_P)^2 + 4K_A C_P\}^{1/2}}{2K_A} \quad 5.$$

and equals the unbound blood concentration $C_{B,u}$ in absence of red cell concentrative mechanisms. The characteristic dependence of the unbound fraction on the K_A and protein concentration for the binding isotherms is depicted in Figure 7. At low K_A, the binding isotherm changes only slightly and gradually with concentration. At high K_A ($> 10^5$ M^{-1}) where binding is

tight, low unbound fractions are seen at low concentration. However, sharp and precipitous increases occur in unbound fraction with small increments of the drug concentration at various regions of the binding isotherms, which appear to be dependent on K_A and the protein concentration (Figure 7, A and B). These marked changes in binding occur when binding is near its saturation capacity such that further small increments in concentration will cause sharp rises in the unbound fractions.

The unbound concentration is often expressed relative to the total plasma concentration, C_P, as an unbound fraction, f_P.

$$f_P = \frac{C_{P,u}}{C_P} \qquad 6.$$

The unbound fraction in blood, f_B, is related to the unbound fraction in plasma as:

$$f_B = \frac{C_{B,u}}{C_B} = \frac{f_P}{(C_B/C_P)} \qquad 7.$$

where C_B/C_P is the blood to plasma concentration ratio.

The manner in which heterogeneous enzymic systems (one, two, and three parallel enzymic systems) modify the unbound fraction along the length of the sinusoid ($f_{B,x}$) has recently been studied (126). From mass balance considerations, the change of the concentration (dC_x) of a flow-limited substrate over a small increment of length, dx, across the single-pass liver preparation at steady-state is described by the following equation:

$$\frac{Q\,dC_x}{dx} = -\frac{1}{L}\sum_{i=1}^{n}\left\{\frac{V_{max,x}^{mi} f_{B,x} C_x}{K_m^{mi} + f_{B,x} C_x}\right\} \qquad 8.$$

where i is the dummy variable for the number of parallel metabolic pathways, and n is 1, 2, or 3; $f_{B,x}$ is the unbound fraction in blood at point x, which, when multiplied by the corresponding substrate concentration, C_x, yields the unbound substrate concentration; $V_{max,x}^{mi}$ and K_m^{mi} are the enzymatic constants for formation of the metabolite, mi, at x. For n multiple metabolic pathways, the rate of loss of substrate at any point x is the sum of the rates of

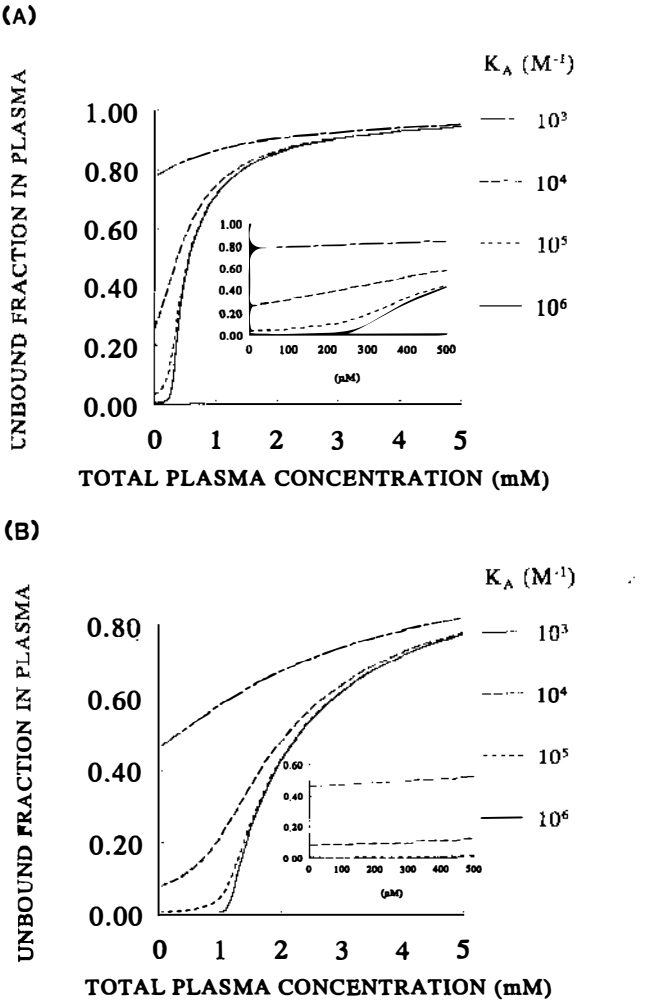

Figure 7 Unbound fraction in plasma *vs* total plasma substrate concentration for the binding of a drug to a single class of two equivalent binding sites. The K_A values are varied from 10^3 to 10^6 M^{-1} at total albumin concentrations of 1% (A) and 4% (B).

formation of the terminal metabolites. As can be seen, with high V_{max}s and low K_ms, removal of the unbound substrate will be greatly facilitated and will further modify the unbound fraction along the length of the sinusoid.

At constant protein concentration, the binding constant, K_A, strongly influences in E_{ss} and f_B between the inlet to the outlet of the liver, or the % change f_B [defined as $(f_{B,In}-f_{B,Out})/f_{B,In} \times 100\%$ where subscripts In and Out

respectively denote the inlet and outlet of the liver sinusoid] for a given enzymic system (same K_m and V_{max}) (Figure 8). For the low K_A (10^3 M^{-1}), E_{ss} displays its characteristic decrease with increasing concentration due primarily to saturation of the enzymic system; the effect of protein binding on metabolism is minimal (Figure 8). For the higher K_A (10^6 M^{-1}), E_{ss} first shows an uncharacteristic increase with concentration, then the pattern shifts to a decreasing trend with concentration (Figure 8). The upward trend of E_{ss} is expected to occur only for tightly bound drugs that are relatively highly cleared, when the availability of unbound drug becomes rate-limiting. However, with increasing concentration, saturation of binding sites (as shown in Figure 7) ensues, causing disproportionately greater increments in unbound drug and unbound fraction; the corresponding % change f_B between the inlet and outlet of the liver becomes greatly magnified (> 100-fold) compared to the lower K_As (cf Figure 8). Thus the rate-limiting step switches to one of the enzymic system (K_m and V_{max}) with increasing concentration. Any further increase in concentration brings about saturation of the enzyme system, and E_{ss} subsequently becomes decreased.

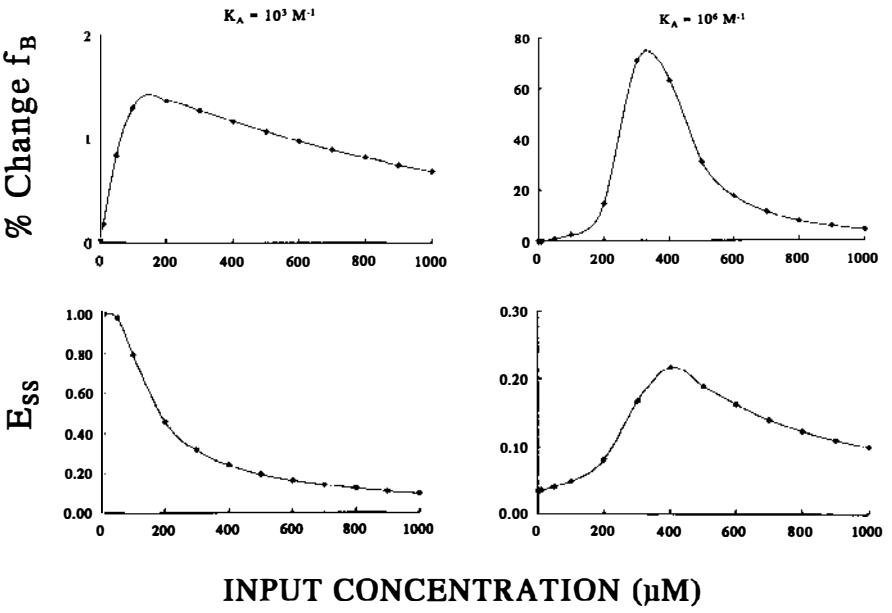

Figure 8 Changes in unbound fraction in blood between the inlet and outlet of the liver (% change in f_B) and the corresponding extraction ratios (E_{ss}) at 1% albumin concentration *vs* C_{In}, for an unienzyme system for binding constants of $K_A = 10^3$ (left panel) and 10^6 (right panel) M^{-1}. The patterns are the same regardless of the distribution of enzymes (data from ref. 126, with permission).

The distribution pattern of a unienzyme system exerts very little or no effect on the overall E_{ss} and the % change f_B (all patterns are the same as seen in Figure 8). However, the unbound fraction at point x along the length of the sinusoid ($f_{B,x}$) differs accordingly for each enzymic distribution pattern. The difference is negligible for low K_A (10^3 M^{-1}) compounds, but is demonstrable for compounds with high binding affinities ($K_A = 10^6$ M^{-1}) (Figure 9). For multiple metabolic systems, small changes in E_{ss} and % change f_B due to variations in enzymic distributions have been detected for simulated data (126). The changes are attenutated when the K_m is increased, and magnified when V_{max} is increased (126).

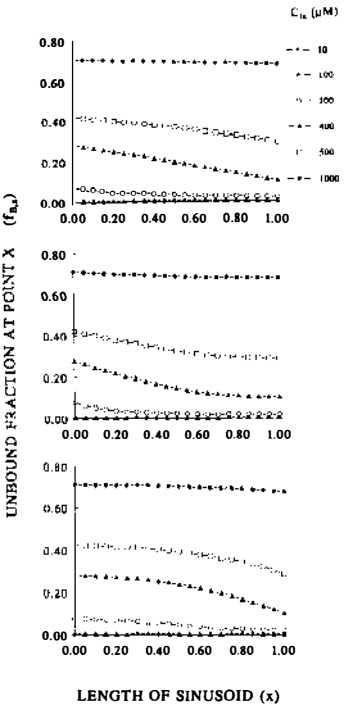

Figure 9 Simulated unbound fraction in blood at point × ($f_{B,x}$) along the length of the sinusoid for a drug that is metabolized by an unienzyme enzyme system at various input concentrations. The K_m (10 uM) and total enzymatic activity (V_{max} or 500 nmol/min) were held constant while the enzymatic activity at different point of x, $V_{max,x}$, is allowed to vary along the sinusoidal flow path (from x=0 to x=L). The change in unbound fraction, $f_{B,x}$ for the K_A of 10^6 M^{-1} are shown for the following distributions: enzyme is evenly distributed (upper panel); enzymic concentration gradient is descending linearly, from a high value at x=0 to zero at x=L (middel panel); enzymic concentration gradient is ascending linearly, from zero at x=0 to a high value at x=L (lower panel). Data for the K_A of 10^3 M^{-1} showed little or no change in $f_{B,x}$ (data from ref. 126, with permission).

Transmembrane Barrier

The general mode of transport of a lipophilic substrate into cells is via passive transport through the liver cell membrane. When the rate of drug permeation into the liver is faster than the rate of delivery by organ perfusion rate, perfusion limitation exists. Alternately, membrane limitation occurs when carrier-mediated mechanisms (127–143) or retardation of polar compounds is present (144), often posing as the rate-controlling factor in the overall uptake when the flux across the membrane is slower than the rate of delivery of substrate by flow. For compounds such as bile acids (131, 132, 134–136,138), organic anions such as bilirubin, indocyanine green, bromosulfophthalein (139–141), neutral compounds such as ouabain (133), and cations such as morphine and nalorphine (142), such carrier systems exist in the liver to facilitate their transport into hepatocytes. Similarly, a carrier system transports glutathione out of liver cells (145). Diffusion rate-limited transport pertains to methotrexate (146), actinomycin D (147), salicylate (148), sulfate and glucuronide conjugates (98,149,150), glutathione conjugates (151), and enalaprilat (152–154), compounds that are of high polarity or exist in the charged or ionized forms at physiological pH.

Membrane limitation on the overall rate of hepatic uptake implies that the transmembrane clearance (permeability surface area product) is smaller than liver blood flow and the hepatic intrinsic clearance, and the unbound drug in sinusoid no longer reflects that in tissue. The effect of a transmembrane barrier on drug extraction may be pictorially depicted (same as preformed metabolite, Figure 10A). The transmembrane clearance CL^d has little effect on E_{ss} for poorly cleared drugs ($CL^d/Q > CL_{int}/Q$). In this case, overall drug removal is dictated by the poor inherent ability within cells (or the intrinsic clearance or CL_{int}) and not by the arrival of substrate through membrane permeation (CL^d). By contrast, the extraction ratios of high intrinsic clearance compounds ($CL_{int}/Q > 10$) is dramatically modulated by membrane permeation. This phenomenon may be readily explained by considering that the rate-controlling step in elimination is not the enzymatic or excretory capacity, but permeation through the membrane. The steady-state expression that describes the rate of change of drug along the length of the liver is given as,

$$\frac{QdC_x}{dt} = - \frac{f_{B,x} C_x CL_x^d CL_{int,x}}{L (CL_{int,x} + CL_x^d)} \qquad 9.$$

where CL_x^d and $CL_{int,x}$ are the transmembrane and intrinsic clearances at point x, respectively.

The manner in which the presence of a transmembrane barrier influences vascular and intracellular events has only recently been illustrated (64–66).

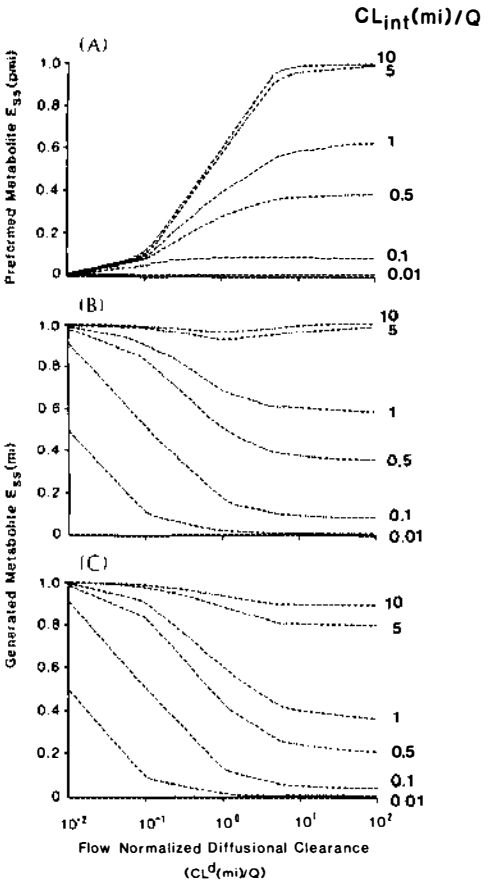

Figure 10 Simulation of the effects between the flow (Q)-normalized transmembrane clearances of drug (CL^d/Q) and metabolite ($CL^d\{mi\}/Q$), and the flow-normalized intrinsic clearances of drug (CL_{int}/Q) and metabolite ($CL_{int}\{mi\}/Q$) on the extraction ratio of a performed ($E_{ss}(pmi)$), (A), and generated metabolite ($E_{ss}(mi)$), (B) and (C). Values of drug intrinsic clearance and transmembrane clearance were varied: CL_{int}/Q values were 10, 5, 1, 0.5, 0.1, 0.01, of which 50% is assumed to conduce to metabolite formation; CL^d/Q were 10^2, 10^1, 10^0, 10^{-1} and 10^{-2} (not all simulations are shown). (A) The steady-state hepatic extraction ratio of preformed metabolite, $E_{ss}(pmi)$, is independent of clearance parameters of drug, but increases with $CL^d\{mi\}/Q$, especially when the metabolite is reasonably highly cleared ($CL_{int}(mi)/Q >> 1$). (B) $E_{ss}(mi)$ decreases with increasing $CL^d\{mi\}/Q$ due to rapid efflux of metabolite into sinusoids, and is altered only slightly by drug parameters, CL_{int} and CL^d. Similar trends are seen for $CL_{int}/Q = 10$ when $CL^d/Q = 100$ or 10. (C) Similar trends in $E_{ss}(mi)$ is seen for $CL_{int}/Q = 0.01$ and $CL^d/Q = 10^{-2}$. The shapes of the graphs are not altered when the % formation is altered (from 50% to 10 or 100%). The numbers adjacent to each graph represent the flow-normalized intrinsic clearance of the metabolite, $CL_{int}(mi)/Q$ (taken from ref. 153, with permission).

The probability of a metabolite encountering membrane-barriers for permeation is even greater than for drug since drug biotransformation usually furnishes metabolites of higher polarity than the parent compound to facilitate excretion. This is readily demonstrated for drug conjugates such as sulfates and glucuronides, which are transferred polar functional groups (98, 149, 150), and the glutathione adduct of styrene oxide (151). Another example is enalaprilat, a dicarboxylic acid metabolite formed from esterolysis of enalapril, an angiotenison converting enzyme inhibitor (152, 154, 155).

Membrane barrier effects on metabolite formation and further elimination have also been examined recently (152, 153). The steady-state expression for the rate of change of a generated metabolite is given by the following expression:

$$\frac{QdC_x(mi)}{dx} =$$

$$-\frac{CL^d(mi)}{L}\left\{\frac{f_{B,x}(mi)C_x(mi)CL_{int,x}(mi) - [CL_x^d f_{B,x}C_x h_{mi,x}CL_{int,x}/(CL_x^d + CL_{int,x})]}{[CL_x^d(mi) + CL_{int,x}(mi)]}\right\} \quad 10.$$

where C_x and $C_x(mi)$ are the concentrations of drug and generated metabolite in sinusoidal blood at any point x, respectively; $f_{B,x}$ and $f_{B,x}(mi)$ correspond to the unbound fractions of drug and metabolite in blood at point x; $h_{mi,x}$ is the fractional intrinsic clearance at point x for mi formation, and when multiplied to the total intrinsic clearance $CL_{int,x}$ at x, the product yields the formation intrinsic clearance of mi at x; $CL_{int,x}(mi)$ is the total intrinsic clearance for the elimination of mi at x. CL_x^d and $CL_x^d(mi)$ denote the transmembrane clearances for drug and metabolite at point x, respectively; Q is the total hepatic flow rate, and L is the length of the sinusoid.

The single-pass perfused rat liver, with concomitant adminstration of differentially labeled drug and its preformed metabolite, has been found to illustrate fully the differential barrier effects on the varying fates between preformed and generated metabolites. This experimental condition is deemed optimal inasmuch as it precludes recirculation of the venous outflow of the formed metabolite, which would behave identically to the preformed metabolite upon re-entry to the liver. The design readily identifies the barrier effect on the removal of both the generated and preformed metabolites. For a generated metabolite, a barrier prevents metabolite efflux and causes the intracellular accumulation of the generated metabolite. Accumulation of the generated metabolite thus exerts a steering effect towards elimination, either

by excretion or metabolism. For the preformed metabolite, the membrane barrier poses as a transport barrier that retards entry, preventing removal of the preformed species.

The steady-state extraction ratios of a preformed vs a generated metabolite may be pictorially represented (Figure 10). The presence of a membrane barrier on a preformed metabolite (similar for drug) retards its removal (displayed as the hepatic extraction ratio E_{ss}(pmi)), especially when the intrinsic clearance of the metabolite is high. E_{ss}(mi), the extraction ratio of the formed metabolite shows almost an inverse relationship with CL^d(mi), the transmembrane clearance of the metabolite, and is additionally influenced by CL_{int}(mi) and precursor parameters, CL_{int} and CL^d, albeit to lesser degrees (Figure 10, B and C). Given the same CL_{int}(mi), decreases in CL^d(mi) will retard preformed metabolite entry and reduce the hepatic extraction ratio of the preformed metabolite (E_{ss}(pmi)) (Figure 10A). A general statement may be made on metabolite extraction and transmembrane barrier for the metabolite: In absence of a barrier (CL^d(mi)/Q is large), E_{ss}(pmi), the extraction ratio of the preformed metabolite is greater than E_{ss}(mi), the extraction ratio of a formed metabolite. This observation has been explained previously as the kinetic phenomenon in sequential metabolite formation. With the presence of a transmembrane barrier, E_{ss}(mi) exceeds E_{ss}(pmi). Indeed, for enalaprilat and acetaminophen sulfate, these polar metabolites are excreted to greater extents as generated metabolites than as the administered, preformed species in single-pass liver perfusion studies (Table 2), despite the similarities in transport and excretory mechanisms for each metabolite entity.

Interplay of Biochemical and Physiological Determinants on Drug and Metabolite Disposition

As seen from the above description, drug and metabolite processing is a distributed-in-space phenomenon. The phenomenon may be used to explain

Table 2 Effect of a transmembrane barrier on the extent of biliary excretion of preformed vs formed metabolites

Polar metabolite	$E(M_1)$[a]	$E(M_1,P)$[b]
Enalaprilat	0.053	0.256[c]
Acetaminophen sulfate	0.003[d]	0.03[e]

[a] extraction ratio of the preformed, administered metabolite
[b] extraction ratio of the formed metabolite, after administration of precursors
[c] Enalapril was the precursor, P (data taken from Ref. 155)
[d] Data taken from Ref. 98
[e] Acetaminophen was the precursor, P (data taken from Ref. 79)

the kinetic lag for the metabolism of a generated metabolite vs the metabolism of its preformed counterpart, disproportionate, downstream metabolite formation due to the modulation by an anterior pathway among parallel pathways, and the effect of hepatic blood flow on downstream metabolite formation. Heterogeneities in enzyme distribution will further modify these differences. Membrane limitation and protein-binding effects are shown as rate-determining factors for metabolite formation and disposition.

These determinants have been studied in isolation or combination, under steady-state conditions, with the single-pass perfused liver preparation. Studies with pulse injection of labeled substrate and metabolite, together with noneliminated reference indicators, have been used to identify barrier-limited entry (128, 129, 143, 149, 150, 154), red cell (87, 88) and plasma and tissue protein binding effects (8–10, 96), cellular distribution, and saturation in removal (128, 129) in the dog liver and in the perfused rat liver preparations. The departure from steady-state in this multiple indicator dilution technique reveals the same, if not more, information on the structure of the liver in drug and metabolite handling. However, the mathematical treatments for these steady-state and non steady-state methods, which incorporate heterogeneity factors and the distributed-in-space phenomenon, have not been applied to the in vivo situation where there is recirculation.

Metabolite Biliary Clearances

As yet, the detailed modeling that describes the control of many of the biological processes in a distributed-in-space fashion (enzyme-distributed modeling) has not been extended to describe venous efflux of substrate back to the circulation for re-entry of the liver in the "recirculation mode". The reason is perhaps because much of the detailed mechanisms revealed from steady-state, single-pass studies or studies conducted with the multiple indicator dilution technique are dampened with the time for recirculation. To describe recirculating events, a simplified physiological modeling approach, which views the liver or a tissue/organ as a well-stirred compartment, subcompartmentalized as tissue blood, interstitial space, liver tissue and the bile compartments, has been used to describe metabolite handling upon recirculation of a bolus dose of the drug and preformed metabolite (23). The model (Figure 11) allows for the incorporation of transmembrane barriers, irreversible removal by metabolism or excretion, binding, flow, and volumes, and is able to account for the sequential first-pass effects of formed metabolites within the liver. The model, however, falls short of a quantitative description of the distributed-in-space phenomenon and the influence of enzyme heterogeneity, since each compartment is assumed to be homogeneous and

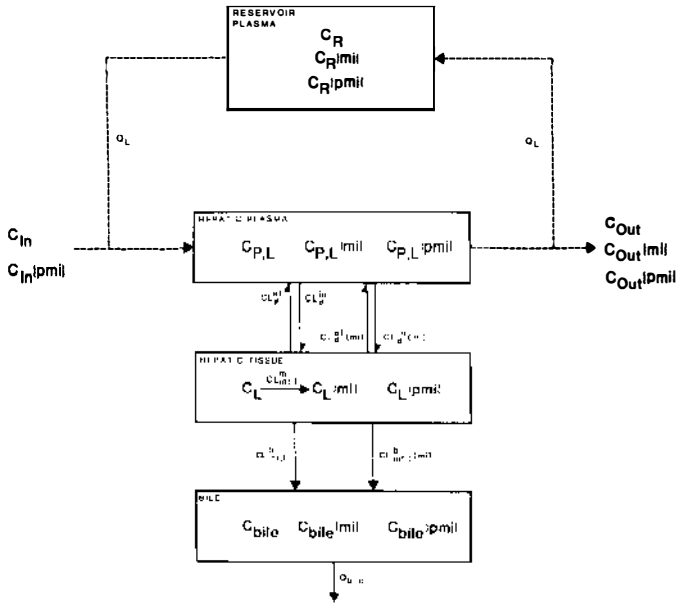

Figure 11 A physiological model for the hepatic elimination of enalapril and enalaprilat (preformed {pmi} and generated {mi}) in the single-pass and recirculating perfused liver preparation. In the single-pass system, constant input concentrations of drug (C_{In}) and preformed metabolite (C_{In}{pmi}) are delivered to the liver at constant flow (Q_L). The liver is divided into three compartments: hepatic plasma, tissue, and bile. Exchange of drug and metabolite between plasma and tissue is characterized by influx (in) and efflux (ef) clearances (CL) across the sinusoidal (*d*) membrane. Drug within tissue is metabolized, by the hepatic metabolic intrinsic clearance, $CL^{mi}_{in,L}$. Biliary excretion of drug and metabolite is a function of bile flow (Q_{Bile}) and the biliary intrinsic clearances, $CL^{b}_{int,L}$ and $CL^{b}_{int,L}$ (mi). Efflux of drug and metabolite in venous outflow is the product of the corresponding outflow concentrations (C_{Out}) and the venous flow rate (Q_L). In the recirculating system, outflow plasma recirculates to a reservoir; drug and metabolite (preformed and generated) concentrations in the reservoir (C_R, C_R{pmi} and C_R{mi}, respectively) represent the input concentrations delivered to the liver (data from ref. 23).

well-mixed. Nonetheless, results from both single-pass delivery and recirculation of injected doses of [^{14}C]enalapril and [^{3}H]enalaprilat with this method suggest a membrane barrier-limitation for the liver cell entry of enalaprilat: E_{ss}(pmi) being less than E_{ss}(mi) in single-pass studies (Figure 12), and accumulation of [^{14}C]enalaprilat upon recirculation of [^{14}C]enalapril (Figure 13). Thus, this simplified model can identify the rate-limiting step in describing the uni-enzyme metabolism of a drug (enalapril) and the excretion of the metabolite (enalaprilat).

The results from the single-pass and recirculating liver experiments of drug

and preformed metabolite have also led to another observation (23). Since enalapril solely forms enalaprilat, which is only biliarily excreted, the biliary clearance of the formed and preformed enalaprilat may be compared. While the biliary excretion clearance of preformed [^{3}H]enalaprilat in recirculation readily reaches a constant value (similar to that in single-pass experiments), the excretion clearance of formed [^{14}C]enalaprilat is time-dependent and higher. With [^{14}C]enalapril becoming depleted with perfusion time, the biliary clearance of the [^{14}C]enalaprilat then approaches that for preformed [^{3}H]enalaprilat. This observation is based on the time-dependency for the dual contributors for excretion: the intracellularly formed and the [^{14}C]enalaprilat in the systemic circulation, since the expression normally applied for estimation of the apparent biliary excretion clearance of the metabolite is given by,

$$CL_{b,app}(mi) = \frac{\text{excretion rate of formed metabolite}}{\text{midpoint concentration of formed metabolite}}$$

$$= \frac{\text{excretion rate of [intracellular + circulating] metabolite}}{\text{midpoint concentration of formed metabolite}} \quad 11.$$

With perfusion time in the recirculating system, less metabolite production occurs and the intracellular component becomes smaller. When the drug is no longer present, the biliary clearance of the formed metabolite is attributed mainly to the circulating [^{14}C]enalaprilat, which is handled identically to that for preformed [^{3}H]enalaprilat (Figure 13).

METABOLITE KINETICS IN THE PRESENCE OF OTHER PARALLEL METABOLITE FORMATION ORGANS: LIVER AND KIDNEY

The liver and kidney, which receive parallel arterial blood supplies, are major organs responsible for the elimination of most xenobiotics. The interorgan relationships between the liver and kidney has recently been studied with a physiological model (Figure 14) and the rat liver and kidney preparations, perfused in parallel with a red cell-albumin medium (156). Again, the precursor [^{14}C]enalapril-product [^{3}H]enalaprilat pair has been used to illustrate these principles, since both the liver and kidney form enalaprilat from enalapril, then both species are excreted into bile and urine. After administration of the loading doses and continuous infusions of [^{14}C]enalapril and preformed [^{3}H]enalaprilat into the reservoir, steady-state conditions are readily achieved

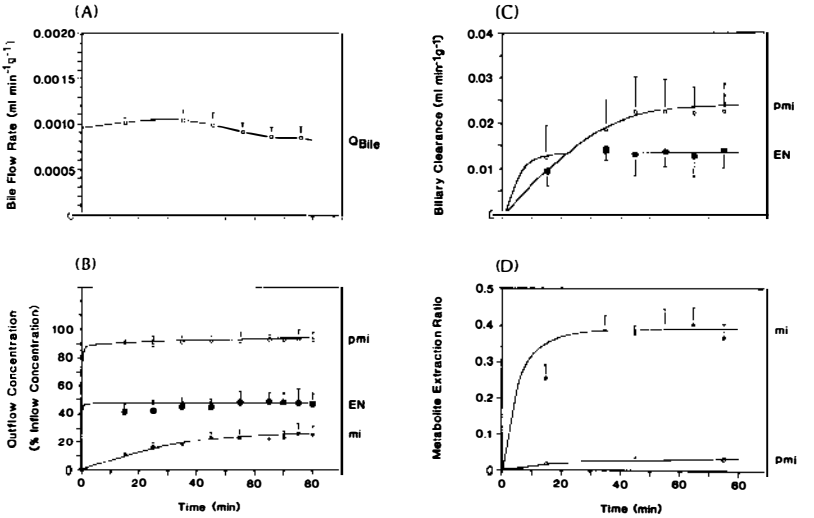

Figure 12 Hepatic handling of simultaneously delivered tracer concentrations of [^{14}C]enalapril and preformed [^{3}H]enalaprilat in the single-pass in situ perfused liver, perfused at 10 ml min^{-1}. (A) The observed bile flow rat (Q_{Bile}) was interpolated by a cubic spline for use in the fitting procedure. (B) The venous plasma concentration-time profiles for [^{14}C]enalapril (EN; closed circles), generated [^{14}C]enalaprilat (mi; closed diamonds) and preformed [^{3}H]enalaprilat (pmi; open diamonds); outflow concentrations are expressed as % inflow concentration. (C) Biliary excretion clearances of [^{14}C]enalapril and preformed [^{3}H]enalaprilat and (D) metabolite extraction ratio for preformed and intrahepatic enalaprilat. The symbols have the same meaning as in (B). The observed data (symbosl, mean±S.D., n=5) and the fitted data (lines) predicted by the model are shown (data from ref. 23).

for [^{14}C]enalapril and [^{3}H]enalaprilat in the reservoir, but not for the formed metabolite, [^{14}C]enalaprilat, which continues to accumulate (Figure 15C). For the administered species [^{14}C]enalapril and [^{3}H]enalaprilat, their biliary clearances and fractional excretion FE (unbound urinary clearance/glomerular filtration rate) are similar to those obtained for the recirculating liver and kidney, respectively: net reabsorption for enalapril and net filtration for preformed enalaprilat (156, 157). The biliary clearance and fractional excretion values of the formed [^{14}C]enalaprilat (FE are greater than those for [^{3}H]enalaprilat, decreasing with perfusion time, after an initial increase (Figure 15, D and E). The trends, very similarly displayed by both the kidney and liver (Figure 15, D and E), indicate that these organs are metabolite formation and excretion organs (19, 23, 156, 157), and reveal the duality of the origins of the excreted species (Eq. 11).

When the condition of combined, recirculating perfusion is simulated with a physiological model (Figure 14), which effectively combines the liver and

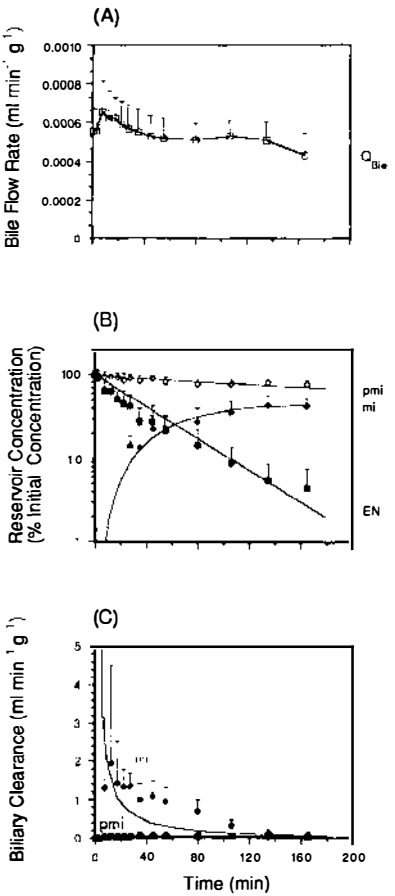

Figure 13 Time profiles for [^{14}C]enalapril (EN; solid circles), generated [^{14}C]enalaprilat (mi; solid diamonds) and preformed [^{3}H]enalaprilat (pmi; open diamonds) upon simultaneous addition of a tracer bolus dose of [^{14}C]enalapril and preformed [^{3}H]enalaprilat to the reservoir of the recirculating rat liver, perfused at constant flow rat (10 ml min^{-1} liver^{-1}). (A) The observed bile flow rate (Q_{Bile}) was interpolated by a cubic spline (line) for use in the simulation. (B) Reservoir plasma concentrations, expressed in terms of perfusate plasma concentration at time=0 post injection. (C) Biliary clearances. The observed data (symbols, mean±S.D., n=6) and the simulated data (line) are shown (data from ref. 23).

kidney models, the metabolic clearance and/or biliary and urinary excretion clearances of preformed enalapril and preformed enalaprilat again show no change for the liver alone, or in presence of the kidney; the converse also holds true. However, for the formed metabolite arising from drug, there is a faster and greater accumulation of metabolite in reservoir for the combined liver-kidney preparation over the isolated kidney and liver preparations, due

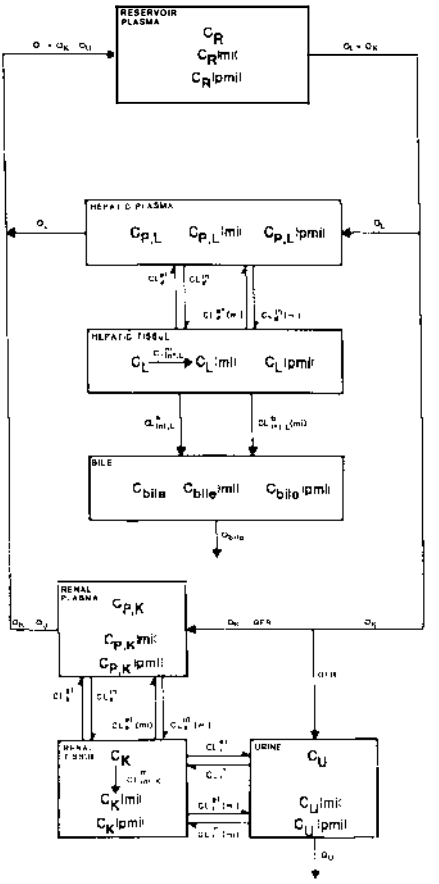

Figure 14 A physiological model for renal and hepatic elimination of enalapril and enelaprilat (preformed {pmi} and generated {mi}) in the combined perfusion of the rat liver and kidney (LK). Reservoir concentrations of drug (C_R) and preformed (C_R{pmi}) and generated (C_R{mi}) metabolites are delivered to the liver and kidney at constant plasma flows (Q_L and Q_K, respectively). The liver is divided into three compartments as in Figure 11. The exchange of drug and metabolite between hepatic plasma and tissue is characterized by influx (in) and efflux (ef) clearances (CL) across the sinusoidal (*d*) membrane. Drug within hepatic tissue is metabolized, with a hepatic metabolic intrinsic clearance, $CL'^{m}_{int,L}$. Biliary excretion of drug and metabolite is a function of bile flow (Q_{Bile}) and the biliary intrinsic clearances, $CL^{b}_{int,L}$ and $CL^{b}_{int,L}$ {mi}. The efflux rate of drug and metabolite in venous outflow is the product of the corresponding hepatic outflow concentrations (C_{Out}) and the venous flow rate (Q_L). The kidney, receiving a parallel arterial supply (Q_K) from the reservoir (data from ref. 156, with permission).

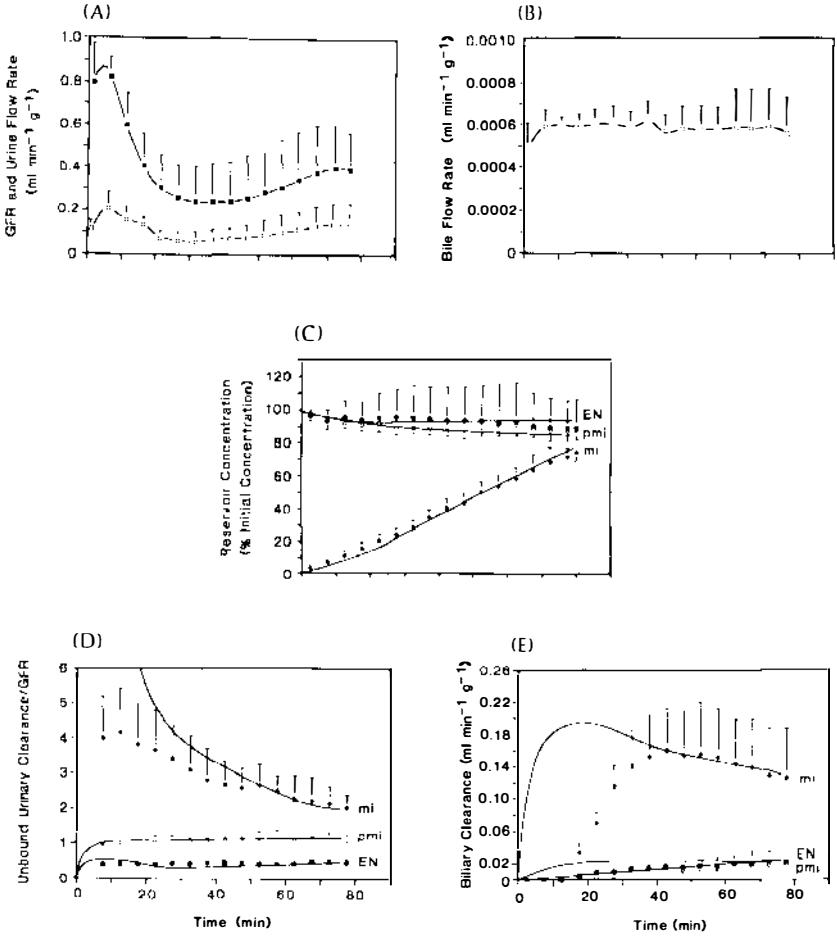

Figure 15 Experimentally observed data (symbols) and simulated curves (lines) predicted by the model for [^{14}C]enalapril (EN; solid circles), its generated metabolite, [^{14}C]enalaprilat (mi; solid diamonds), and preformed [^{3}H]enalaprilat (pmi; open diamonds), after administration of a loading dose and constant infusion of [^{14}C]cnalapril and [^{3}H]-enalaprilat to the reservoir of the combined, recirculating liver and kidney preparation, perfused at 10 ml min^{-1} organ^{-1}. Splined data (lines) for (A) the observed GRF (solid squares) and urine flow rates (open squares), and (B) bile flow rates (open squares) were used for simulations. (C) Reservoir plasma concentrations, expressed in terms of perfusate plasma concentration at t=0, (D) the unbound urinary clearances/ GFR (fractional excretions), and (E) biliary clearances were plotted against perfusion time. Data are mean±S.D., n=6, and from ref. 156, with permission.

to the presence of an additional metabolite formation organ (Figure 16A). The biliary (Figure 16B) and urinary (Figure 16C) clearances for the formed metabolite in the combined liver-kidney preparation also differ from those for the liver and kidney preparations, respectively. In the presence of another metabolite formation organ, greater accumulation of the formed metabolite results in the reservoir; estimation of the apparent excretory (urinary and

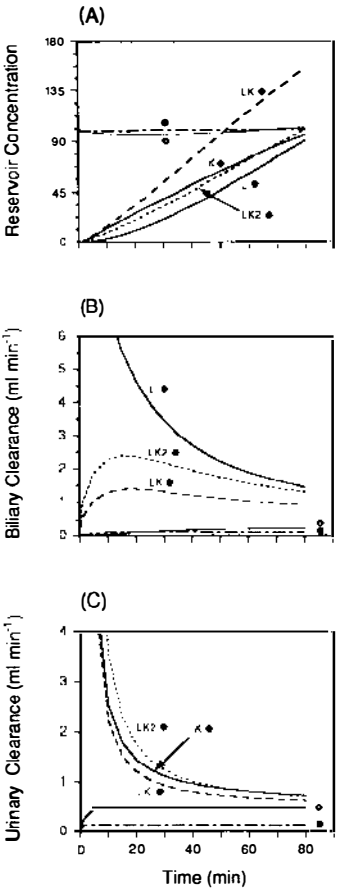

Figure 16 The effects of multiple metabolite formation organ and volume of reservoir on excretion clearances of the formed metabolite. (A) Reservoir plasma concentrations, (B) biliary excretion clearances, and (C) urinary clearance profiles were simulated for [^{14}C]enalapril (solid circles), its generated metabolite [^{14}C]enalaprilat (solid diamonds), and preformed [^{3}H]enalaprilat (open diamonds), after a loading dose and during steady-state infusion of [^{14}C]enalapril and [^{3}H]enalaprilat, in the recirculating liver (L) and kidney (K) perfused in isolation and in the combined perfusion (LK), when all systems are of the same reservoir size, and when LK has double the reservoir size (LK2) (data from ref. 156, with permission).

biliary) clearance of the formed metabolite in liver-kidney preparation by Eq. 11 will yield lower values than those projected for liver or kidney alone. With a doubling of the reservoir size for the liver-kidney preparation, a condition tantamount to a dilution of the accumulated concentration of the formed metabolite in the reservoir, a rise in the apparent metabolite clearance follows. The presence of other metabolite formation organs and the size of the distribution volume thus alter estimates of the apparent excretory clearances of the formed metabolite, but not for the preformed species: drug or preformed metabolite.

METABOLITE KINETICS IN THE PRESENCE OF OTHER SERIAL METABOLITE FORMATION ORGANS: LIVER AND INTESTINE

The intestine, liver, and lung are three drug-metabolizing organs involved in the first-pass effect of orally administered substrates. Because of the anatomical placement of these organs, the intestine, being anterior, reduces the flux of substrate entering the liver and, in turn, the contribution of hepatic, then lung metabolism in the overall first-pass effect (158–162). Intestinally formed metabolites may themselves serve as substrates for further hepatic metabolism prior to their reaching the general circulation. Although the first-pass effect of a drug and its overall assessment are well established, the role of the intestine and liver in metabolite formation and consecutive metabolism during first-pass and subsequent passes needs appraisal, inasmuch as the nature and proportions of metabolites formed differ between these first-pass organs.

The segregation of intestinal and hepatic metabolism in the first-pass effect has been studied by both perfusion and in vivo experiments (160, 163–170). The first-pass effect by the intestine and liver has been approached by a single-pass rat small intestine-liver preparation, with drug entering the superior mesenteric artery, and blank perfusate into the hepatic artery (hepatic arterial flow is 33% of intestinal blood flow and 25% of total liver blood flow) (168–170). The steady-state extraction ratios of the intestine, E_I, and liver, E_H, and the contribution of each tissue/organ in first-pass metabolism may be segregated in this system. The rate of elimination divided by the rate of presentation at steady state provides the individual extraction ratios:

$$E_I = \frac{Q_{PV}(C_{SMA} - C_{PV})}{Q_{PV}C_{SMA}} = 1 - \frac{C_{PV}}{C_{SMA}} \qquad 12.$$

$$E_H = \frac{Q_{PV}C_{PV} - Q_{HV}C_{HV}}{Q_{PV}C_{PV}} = 1 - \frac{Q_{HV}C_{HV}}{Q_{PV}C_{PV}} = 1 - 1.333\,\frac{C_{HV}}{C_{PV}} \qquad 13.$$

where C_{PV}, C_{SMA}, C_{HA} and C_{HV} denote the steady-state drug concentrations in the portal vein, superior mesenteric artery, hepatic artery, and hepatic vein, respectively; Q_{HV}, Q_{PV} and Q_{HA} represent the hepatic venous, portal venous, and hepatic arterial flows, respectively. The ratio of flow rates, Q_{HV}/Q_{PV} or 1.333 (10/7.5), is the dilution factor of hepatic venous blood by the drug-free hepatic artery. Since there is no drug presented to the hepatic artery ($C_{HA} = 0$), the effective extraction across the intestine and liver (E_{IL}) is:

$$E_{IL} = \frac{Q_{PV}C_{SMA} - Q_{HV}C_{HV}}{Q_{PV}C_{SMA}} = 1 - 1.333\,\frac{C_{HV}}{C_{SMA}} \qquad 14.$$

When the metabolites formed from the intestine and liver are conjugates that do not undergo further metabolism in both the intestine and liver, the steady-state formation rate of conjugates for the intestine (v_I^{mi}) may be found as the product of portal venous flow (Q_{PV}) and the steady-state portal venous concentration of the metabolite (C_{PV}(mi)), plus the time-averaged appearance rate of mi into lumen (amount recovered divided by time for collection, $\Delta A_{lumen}/\Delta t$) (168):

$$v_I^{mi} = Q_{PV}C_{PV}(mi) + \frac{\Delta A_{lumen}(mi)}{\Delta t} \qquad 15.$$

Since the hepatic venous concentration of the conjugate mi consists of total metabolite arising from both intestine and liver metabolism, the steady-state hepatic formation rates are obtained as follows:

$$v_H^{mi} = Q_{HV}C_{HV}(mi) + \frac{\Delta A_e(mi)}{\Delta t} - Q_{PV}C_{PV}(mi) - \frac{\Delta A_{lumen}(mi)}{\Delta t} \qquad 16.$$

where v_H^{mi} is the hepatic formation rate for the conjugate mi; $C_{PV}\{mi\}$ and C_{HV}(mi) are the portal and hepatic venous concentrations of the conjugate, respectively; $\Delta A_e(mi)/\Delta t$ is the biliary excretion rate of mi, at steady state.

The contribution of the intestine and liver to the overall elimination is given by the ratio of the rate of intestine or liver metabolism to the total rate of elimination across the two organs, at steady state:

$$\frac{v_I}{v_{total}} = \frac{E_I Q_{PV} C_{SMA}}{(E_I C_{SMA} + E_H C_{PV}) Q_{PV}} = \frac{E_I}{E_I + E_H(1 - E_I)} \quad 17.$$

$$\frac{v_H}{v_{total}} = \frac{E_H Q_{PV} C_{PV}}{(E_I C_{SMA} + E_H C_{PV}) Q_{PV}} = \frac{E_H(1 - E_I)}{E_I + E_H(1 - E_I)} \quad 18.$$

The individual contribution of the intestine and liver to each conjugation pathway in the first-pass effect may be further expressed in terms of the total conjugation rate for each conjugate:

$$\text{contribution by intestine} = \frac{v_I^{mi}}{v_I^{mi} + v_H^{mi}} \times 100\% \quad 19.$$

$$\text{contribution by liver} = \frac{v_I^{mi}}{v_I^{mi} + v_H^{mi}} \times 100\% \quad 20.$$

The influence of the intestine on the fraction of total, first-pass elimination that is hepatic at different E_H values (from 0 to 1) is depicted (Figure 17). No hepatic elimination occurs when E_I was 1.0 regardless of the values of E_H (the bottom horizontal line), when the substrate is completely removed prior to

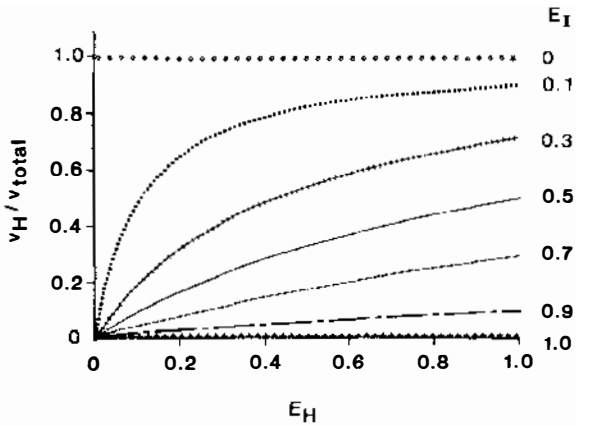

Figure 17 The influence of intestinal extraction ratios on the contribution of the liver to overall metabolism at different hepatic extraction ratios (data from ref. 168, with permission).

reaching the liver. As E_I decreases, more hepatic elimination becomes noticeable. The intestine, the anatomically anterior tissue, is first to encounter any portally absorbed compound. It regulates the available substrate for hepatic metabolism and hence reduces the contribution of hepatic metabolism to the total first-pass effect (168). In analogy to the competing, parallel conjugative pathways within the liver, the intestine will greatly modify the contribution of liver metabolism to the first-pass effect due to its ability to deplete substrate (162).

Typically, intestinal metabolism plays a more significant role in first-pass metabolism at low substrate concentrations reaching the superior mesenteric artery. With increasing concentration of substrate, saturation of intestinal metabolism occurs, and the impact of intestinal metabolism on first-pass metabolism is reduced. These aspects should be considered in first-pass metabolism when substrates pass successively into the intestine, then the liver (168, 169).

This behavior is exemplified by gentisamide (GAM), which is principally glucuronidated by the intestine and sulfated primarily by the liver. The steady-state extraction ratios of the intestine, E_I (0.33 to 0.06), and liver, E_H (0.84 to 0.37), found according to Eqs. 12 and 13, are highly concentration-dependent, decreasing with GAM concentrations (Figure 18); there were with concomitant decreased contributions of intestinal glucuronidation (and to a lesser extent, sulfation) to the total (sum of intestine and liver) glucuronidation (or sulfation) rate (Figure 19; 169). Similar trends have been observed for

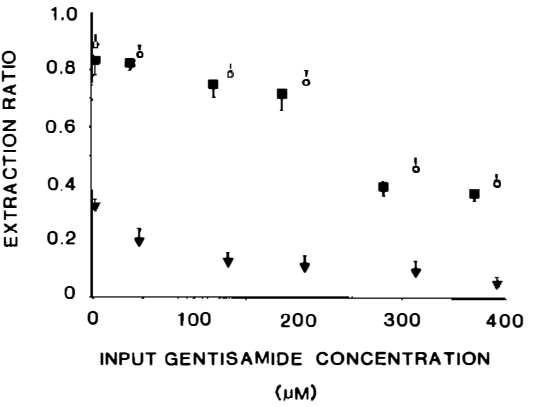

Figure 18 The interrelationships among extraction ratios for the intestine, E_I (▲), liver, E_H(■), and the effective extraction ratio across the lintestine and liver, E_{IL} (○) with varying input gentisamide (GAM) concentration to the organs: intestine, liver, and intestine-liver (Eqs. 12–14) (data from ref. 169, with permission).

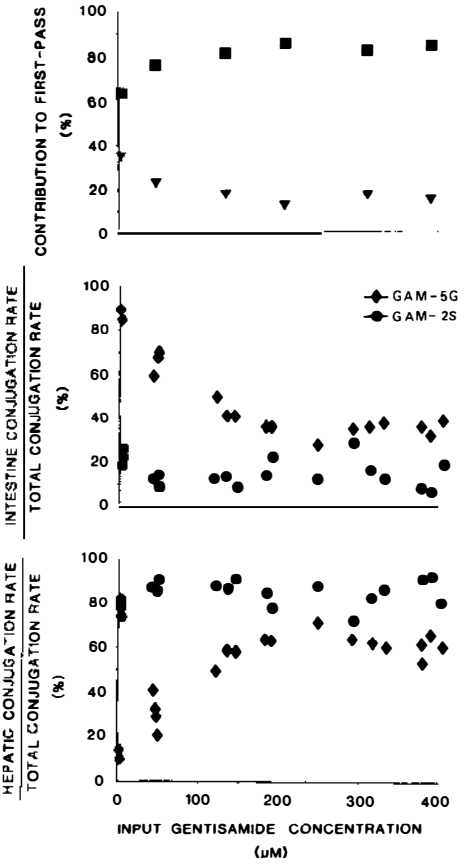

Figure 19 The contribution of the intestine and liver to the overall first-pass metabolism of gentisamide (upper panel, and individual intestinal (middle panel) and hepatic (bottom panel) conjugation (sulfation or glucuronidation) rate divided by the sum of the total rate (sum of intestine and liver) for the conjugative pathway (Eqs. 19, 20), at varying input concentrations of GAM to the intestine-liver. The symbols were: upper panel, (▲) intestine, and (■) liver; middle and bottom panels: (●) GAM-2S, and (♦) GAM-5G (data from ref. 169, with permission).

both salicylamide and 4-methylumbelliferone, which are glucuronidated by the intestine and sulfated by the liver (168, 170).

CONCLUDING REMARKS

The importance of biological variables on hepatic drug and metabolite clearances and the interplay of these determinants in a distributed-in-space fashion have been reviewed, mostly in single-pass liver perfusion studies. As can be

seen, any one of these variables may become rate-limiting, and are highly dictated by the substrate concentration entering the liver. In some instances, it is highly probable that the rate-limiting step for the overall uptake process may change during a single traverse of drug or metabolite across the length of the sinusoid.

The limitation in the prediction of metabolite kinetics in a recirculating system at the present stage of development is restricted to the mere consideration of each organ/tissue or its subcompartments as more simplified, well-mixed compartments, viz, the physiological modeling approach. This approach, though failing to describe the distributed-in-space phenomenon within each eliminating organ or incorporate enzyme heterogeneity in metabolite formation and sequential metabolism, is nevertheless adequate in expressing sequential elimination of metabolites and the rate-limiting step in drug and metabolite uptake.

The field of metabolite kinetics is still at an early stage of development. Its quantitative expression requires the identification of the metabolite formation organ (58, 156) and knowledge of whether sequential elimination occurs within metabolite formation organs or other elimination organs, since differences are expected between serially arranged and parallel, metabolizing organs, as discussed here. The effect of a membrane barrier on sequential metabolism is yet to be explored and is expected to differ between a formation organ and another organ where consecutive metabolism occurs. These complexities, often overlooked when viewing metabolite kinetics, serve as fertile grounds for future exploration.

ACKNOWLEDGMENT

This work was supported by grants from the Medical Research Council, Canada (DG-263, MA-9104, MA-9765), and from the National Institutes of Health, USA (GM-38250).

Literature Cited

1. Collins, J. M., Blake, D. A., Egner, P. G. 1978. Phenytoin metabolism in the rat: pharmacokinetic correlation between in vitro hepatic microsmal enzyme activity and in vivo elimination kinetics. *Drug Metab. Dispos.* 6:251–57
2. Lin, J. H., Hayashi, M., Awazu, S., Hanano, M. 1978. Correlation between in vitro and in vivo drug metabolism rate: oxidation of ethoxybenzamide in rat. *J. Pharmacokin. Biopharm.* 6:327–37
3. Igari, Y., Sugiyama, Y., Sawada, Y., Iga, T., Hanano, M. 1984. In vitro and in vivo assessment of hepatic and extrahepatic metabolism of diazepam in the rat. *J. Pharm. Sci.* 73:826–28
4. Gillette, J. R. 1971. Factors affecting drug metabolism. *Ann. NY Acad. Sci.* 179:43–66
5. Pang, K. S., Rowland, M. 1977. Hepatic clearance of drugs. II. Experimental evidence for the acceptance of the"well-stirred" model over the "parallel tube" model using lidocaine in the perfused rat liver in situ preparation. *J. Pharmacokin. Biopharm.* 5:655–80
6. Pang, K. S., Lee, W-F., Cherry, W. F., Yuen, V., Accaputo, J., et al. 1988. Effects of perfusate flow rate on mea-

sured blood volume, Disse space, intracellular water spaces, and drug extraction in the perfused rat liver preparation: characeterization by the technique of multiple indicator dilution. *J. Pharmacokin. Biopharm.* 16:595–632
7. Fleischner, G., Meijer, D. K. F., Levine, W. G., Gatmaitan, Z., Gluck, R., Arias, I. M. 1975. Effect of hypolipidemic drugs, nafenopin and clofibrate, on the concentration of ligandin and Z protein in rat liver. *Biochem. Biophys. Res. Commun.* 67:1401–7
8. Goresky, C. A., Daly, D. S., Mishkin, D., Arias, I. M. 1978. Uptake of labeled palmitate by the intact liver: role of intracellular binding sites. *Am. J. Physiol.* 234:E542–53
9. Wolkoff, A. W., Goresky, C. A., Sellin, J., Gatmaitan, S., Arias, I. M. 1979. Role of ligandin in transfer of bilirubin from plasma into liver. *Am. J. Physiol.* 236:E638–48
10. Gartner, U., Stockert, R. J., Levine, W. G., Wolkoff, A. W. 1982. Effect of nafenopin on the uptake of bilirubin and sulfobromophthalein by the isolated perfused rat liver. *Gastroenterology* 83: 1163–69
11. Theilmann, L., Stollman, Y. R., Arias, I. M., Wolkoff, A. W. 1985. Does Z-protein have a role in transport of bilirubin and bromosulfophthalein by isolated perfused rat liver? *Hepatology* 5:923–26
12. Pang, K. S., Xu, X. 1988. Drug metabolism factors in drug discovery and design. In *Pharmacokinetics: Regulatory-Industrial-Academic Perspectives,* ed. P. G. Welling, F. L-S. Tse, pp. 383–447. New York: Marcel Dekker
13. Pang, K. S. 1989. Liver perfusion studies on drug and metabolite processing. *Rev. Biochem. Toxicol.* 10:187–263
14. Pang, K. S., St-Pierre, M. V. 1991. Hepatic modeling of drugs and metabolites, In *Progress in Pharmacology and Clinical Pharmacology. Biliary Excretion of Drugs and Other Chemicals,* ed. J. Watkins III, S-P. Siegers, pp. 337–59. Stuttgart/New York: Fischer Verlag
15. Pang, K. S. 1990. Deterministic factors regulating conjugation reactions in eliminating organs. In *Conjugation Reactions in Drug Metabolism: An Integrated Approach,* ed. G. J. Mulder, pp. 5–39. London: Taylor & Francis
16. Chen, R., Gillette, J. R. 1988. Pharmacokinetic procedures for the estimation of organ clearances for the formation of short-lived metabolites. Acetaminophen induced glutathione depletion in hamster. *Drug Metab. Dispos.* 16:373–85
17. Reinke, L. A., Belinsky, S. S., Evans, R. K., Kauffman, F. C., Thurman, R. G. 1981. Conjugation of p-nitrophenol in the perfused rat liver: the effect of substrate concentration and carbohydrate reserves. *J. Pharmacol. Exp. Ther.* 217: 863–70
18. Pang, K. S., Gillette, J. R. 1979. Sequential first-pass elimination of a metabolite derived from its precursor. *J. Pharmacokin. Biopharm.* 7:275–90
19. de Lannoy, I. A. M., Hirayama, H., Pang, K. S. 1990. A physiological model for renal drug metabolism: Enalapril esterolysis to enalaprilat in the isolated perfused rat kidney. *J. Pharmacokin. Biopharm.* 18: 561–88
20. Pang, K. S. 1981. Metabolite pharmacokinetics: The area under the curve of metabolite and the fractional rate of metabolism of a drug after different routes of administration for renally and hepatically cleared drugs and metabolites. *J. Pharmacokin. Biopharm.* 8: 477–87
21. Pang, K. S., Kwan, K. C. 1983. A Commentary. Methods and assumptions in the kinetic estimation of metabolite formation. *Drug Metab. Dispos.* 11:79–84
22. Pang, K. S. 1985. A review of metabolite kinetics. *J. Pharmacokin. Biopharm.* 13:632–62
23. de Lannoy, I. A. M., Barker, F. III, Pang, K. S. 1992. Differences in metabolite excretion clearances in formation organs: Studies with enalapril and enalaprilat in the single pass and recirculating perfused rat liver. *J. Pharmacokin. Biopharm.* In press
24. Rowland, M., Tozer, T. N. 1980. *Clinical Pharmacokinetics. Concepts and Applications.* Philadelphia: Lea & Febiger
25. Gibaldi, M., Perrier, D. G. 1982. *Drugs and The Pharmaceutical Sciences,* Vol. 15. *Pharmakinetics.* New York: Marcel Dekker. 2nd. ed.
26. St-Pierre, M. V., Xu, X., Pang, K. S. 1988. Primary, secondary, and tertiary metabolite kinetics. *J. Pharmacokin. Biopharm.* 16:493–527
27. Schwartz, M. A., Koechlin, B. A., Postma, E., Palmer, S., Krol, G. 1965. Metabolism of diazepam in rat, dog and man. *J. Pharmacol. Exp. Ther.* 149: 423–35
28. Keenaghan, J. B., Boyes, R. N. 1971. The tissue distribution, metabolism, and excretion of lidocaine in rats, guinea

pigs, dogs and man. *J. Pharmacol. Exp. Ther.* 180:454–63
30. Nelson, S. D., Breck, G. D., Trager, W. F. 1973. In vivo metabolite condensations. Formation of N^1-ethyl-2-methyl-N^3-(2,6-dimethylphenyl)- 4-imidazolidinone from the reaction of a metabolite of alcohol with a metabolite of lidocaine. *J. Med. Chem.* 16:1106–12
31. Walle, T., Gaffney, T. E. 1972. Propranolol metabolism in man and dog: Mass spectrometric identification of six new metabolites. *J. Pharmacol. Exp. Ther.* 182:83–92
32. Fenselau, C., Lehman, J. P., Myles, A., Brandt, J., Yost, G. S., et al. 1982. Iminocyclophosphamide as a chemically reactive metabolite of cyclophosphamide. *Drug Metab. Dispos.* 10:636–40
33. Novikoff, A. B. 1959. Cell heterogeneity within the hepatic lobule of the rat (staining reactions). *J. Histochem. Cytochem.* 7:240–44
34. Miller, D. L., Zanolli, C. S., Gumucio, J. J. 1979. Quantitative morphology of the sinusoids in the hepatic acinus. *Gastroenterology* 76:965–69
35. de Leeue, A. M., Knook, D. L. 1984. The ultrastructure of sinusoidal liver cells in the intact rat at various ages. In *Pharmacological, Morphological and Physiological Aspects of Aging,* ed. C. F. A. van Bezooijen, pp. 91–96. Rijswik: Eurage
36. Rappaport, A. M., Borowy, Z. J., Lougheed, W. M., Lotto, W. N. 1954. Subdivision of hexagonal liver lobules into a structural and functional unit: Role in hepatic physiology and pathology. *Anat. Rec.* 119:11–34
37. Rappaport, A. M. 1958. The structural and functional unit in the human liver (liver acinus). *Anat. Rec.* 130:673–89
38. Rappaport, A. M. 1980. Hepatic blood flow: Morphologic aspects and physiologic regulation. In *Liver and Biliary Tract Physiology. I. International Review of Physiology,* ed. N. B. Javitt, 21:1–63. Baltimore: Univ. Park Press
39. Gooding, P. E., Chayen, J., Sawyer, B., Slater, T. F. 1978. Cytochrome P-450 distribution in rat liver and the effect of sodium phenobarbitone administration. *Chem. Biol. Interact.* 20:299–310
40. Jungerman, K., Katz, N. 1982. Functional hepatocellular heterogeneity. *Hepatology* 2:385–95
41. Burger, H. J., Gebhardt, R., Mayer, C., Mecke, D. 1989. Different capacities for amino acid transport in periportal and perivenous hepatocytes isolated by digitonin/collagenase perfusion. *Hepatology* 9:22–28
42. Bass, N. M., Barker, M. E., Manning, J. A., Jones, A. L., Ockner, R. K. 1989. Acinar heterogeneity of fatty acid binding protein expression in livers of male, female, and clofibrate-treated rats. *Hepatology* 9:12–21
43. McFarlane, B. M., Spios, J., Gove, C. D., McFarlane, I. G., Williams, R. 1990. Antibodies against the hepatic asialoglycoprotein receptor perfused in situ preferentially attach to periportal liver cells in the rat. *Hepatology* 11:408–15
44. Thurman, R. G., Kauffman, F. C., Jungermann, K. 1987. *Regulation of Hepatic Metabolism. Intra- and Intercellular Compartmentation.* New York: Plenum
45. Goresky, C. A. 1963. A linear method for determining liver sinusoidal and extravascular volumes. *Am. J. Physiol.* 204:626-40
46. Boyer, J. L., Elias, E., Layden, T. J. 1979. The paracellular pathway and bile formation. *Yale J. Biol. Med.* 52:61–67
47. Gumucio, J. J., Balabaud, C., Miller, D. L., Demason, L. F., Appleman, H. D., et al. 1978. Bile secretion and liver cell heterogeneity in the rat. *J. Lab. Clin. Med.* 91:350–62
48. Rowland, M., Benet, L. Z., Graham, G. G. 1973. Clearance concepts in pharmacokinetics. *J. Pharmacokin. Biopharm.* 1:123–36
49. Pang, K. S., Rowland, M. 1977. Hepatic clearance of drugs. I. Theoretical consideration of a "well-stirred" model and a "parallel tube" model. Influence of hepatic blood flow, plasma and blood cells binding, and the hepatocellular activity on hepatic drug clearance. *J. Pharmacokin. Biopharm.* 5:625–53
50. Winkler, W., Keiding, S., Tygstrup, N. 1973. Clearance as a quantitative measure of structure and function. In *The liver: Quantitative Aspects of Structure and Function,* ed. P. Paumgartner, R. Preisig, pp. 144–55. Basel: Karger
51. Bass, L., Robinson, P., Bracken, A. J. 1978. Hepatic elimination of flowing substrates: The distributed model. *J. Theor. Biol.* 72:161–84
52. Pang, K. S., Stillwell, R. N. 1983. An understanding of the role of enzymic localization of the liver on metabolite kinetics: A computer simulation. *J. Pharmacokin. Biopharm.* 11:451–68
53. Sawada, Y., Sugiyama, Y., Miyamoto, Y., Iga, T., Hanano, M. 1985. Hepatic clearance model: comparison among the distributed, parallel-tube and well-

stirred models. *Chem. Pharm. Bull.* 33:319–26
54. Roberts, M. S., Rowland, M. 1985. Hepatic elimination-dispersion model. *J. Pharm. Sci.* 74:585–87
55. Goresky, C. A. 1980. Uptake in the Liver: The nature of the process. See Ref. 38, pp. 65–101
56. Wilkinson, G. R. 1987. Clearance approaches in pharmacology. *Pharmacol. Rev.* 39:1–47
57. Pang, K. S. 1981. Metabolite pharmacokinetics: The area under the curve of metabolite and the fractional rate of metabolism of a drug after different routes of administration for renally and hepatically cleared drugs and metabolites. *J. Pharmacokin. Biopharm.* 8:477–87
58. Pang, K. S. 1985. A review of metabolite kinetics. *J. Pharmacokin. Biopharm.* 13:632–62
59. St-Pierre, M. V., Lee, P. I., Pang, K. S. 1992. A comparative investigation of hepatic clearance models: predictions of metabolite formation and elimination. *J Pharmacokin. Biopharm.* In press
60. Jones, A. L., Hreadek, G. T., Renston, R. H., Wong, K. Y., Karlagnais, G., Paumgartner, G. 1980. Autoradiographic evidence for hepatic lobular concentration gradient of bile acid derivative. *Am. J. Physiol.* 238:G233–37
61. Gumucio, J. J., Miller, D. L., Krauss, M. D., Zanolli, C. C. 1981. Transport of fluorescent compounds into hepatocytes and the resultant zonal labeling of the hepatic acinus in the rat. *Gastroenterology* 80: 639–46
62. Gumucio, D. L., Gumucio, J. J., Wilson, J. A. P., Cutter, C., Krauss, M., et al. 1984. Albumin influences sulfobromophthalein transport by hepatocytes of each acinar zone. *Am. J. Physiol.* 246:G86–G95
63. Weisiger, R. A., Mendel, C. A., Cavalieri, R. R. 1986. The hepatic sinusoid is not well-stirred: estimation of the degree of axial mixing by analysis of lobular concentration gradients formed during uptake of thyroxinc by the perfused rat liver. *J. Pharm. Sci.* 75:233–37
64. Baron, J., Redick, R. A., Guengerich, F. P. 1982. An immunohistochemical study on the localizations and distributions of phenobarbital- and 3-methylcholanthrene-inducible cytochrome P-450 within the livers of untreated rats. *J. Biol. Chem.* 256:15200–3
65. Baron, J., Redick, R. A., Guengerich, F. P. 1982. Effect of 3-methylcholanthrene, β-naphthoflavone, and phenobarbital on the 3-methylcholanthrene inducible isozyme of cytochrome P-450 within centrilobular, midzonal, and periportal hepatocytes. *J. Biol. Chem.* 257:953–57
66. Taira, Y., Redick, J. A., Baron, J. 1981. An immunohistochemical study on the localization and distribution of NADPH cytochrome c (P-450) reductase in rat liver. *Mol. Pharmacol.* 17:374–81
67. Ullrich, D., Fisher, G., Katz, N., Bock, K. W. 1984. Intralobular distribution of UDP-glucuronosyltransferase in livers from untreated, 3-methylcholanthrene- and phenobarbital-treated rats. *Chem. Biol. Interact.* 48:181–90
68. Knapp, S. A., Green, M. D., Tephly, T. R., Baron, J. 1988. Immunohistochemical demonstration of isozyme- and strain-specific differences in the intralobular localizations and distributions of UDP-glucuronosyltransferases in livers of untreated rats. *Mol. Pharmacol.* 33:14–21
69. Redick, J. A., Jakoby, W. B., Baron, J. 1982. Immunohistochemical localization of glutathione-S-transferase in livers of untreated rats. *J. Biol. Chem.* 257: 15200–3
70. Kawabata, T. T., Guengerich, F. P., Baron, J. 1981. An immunohistochemical study on the localization and distribution of epoxide hydrolase within livers of untreated rats. *Mol. Pharmacol.* 20:709–14
71. Conway, J. G., Kauffman, F. C., Ji, S., Thurman, R. G. 1982. Rates of sulfation and glucuronidation of 7-hydroxycoumarin in periportal and pericentral regions of the liver lobule. *Mol. Pharmacol.* 22:509–16
72. Conway, J. G., Kauffman, F. C., Tsukada, T., Thurman, R. G. 1984. Glucuronidation of 7-hydroxycoumarin in periportal and pericentral regions of the liver lobule. *Mol. Pharmacol.* 25: 487–93
73. Conway, J. G., Kauffman, F. C., Tsukuda, T., Thurman, R. G. 1987. Glucuronidation of 7-hydroxycoumarin in periportal and pericentral regions of the lobule in livers from untreated and 3-methyl-cholanthrene-treated rats. *Mol. Pharmacol.* 33:111–19
74. deBaun, J. R., Smith, J. Y. R., Miller, E. C., Miller, J. A. 1971. Reactivity in vivo of the carcinogen N-hydroxy-2-acetylaminoflourene: Increase by sulfate ion. *Science* 167:184–86
75. Meerman, J. H. N., Mulder, G. J. 1981. Prevention of the hepatotoxic action of N-hydroxy-2-acetylaminofluorene in the

rat by inhibition of N-●-sulfation by pentachlorophenol. *Life Sci.* 21:2361–65
76. Pang, K. S., Koster, H., Halsema, I. C. M., Scholtens, E., Mulder, G. J., Stillwell, R. N. 1983. Normal and retrograde perfusion to probe the zonal distribution of sulfation and glucuronidation activities of harmol in the perfused rat liver preparation. *J. Pharmacol. Exp. Ther.* 224:647–53
77. Morris, M. E., Yuen, V., Pang, K. S. 1987. Competing pathways in drug metabolism. II. Competing pathways in drug metabolism. Enzymic systems for 2- and 5-sulfoconjugation are distributed anterior to 5-glucuronidation in the metabolism of gentisamide by the perfused rat liver. *J. Pharmacokin. Biopharm.* 16:633–56
78. Xu, X., Pang, K. S. 1989. Hepatic modeling of metabolite kinetics in sequential and parallel pathways: salicylamide and gentisamide metabolism in perfused rat liver. *J. Pharmacokin. Biopharm.* 17: 645–71
79. Pang, K. S., Terrell, J. A. 1981. Retrograde perfusion to probe the heterogeneous distribution of hepatic drug metabolizing enzymes in rats. *J. Pharmacol. Exp. Ther.* 216:339–46
80. Pang, K. S., Cherry, W. F., Accaputo, J., Schwab, A. J., Goresky, C. A. 1988. Combined hepatic arterial-portal venous or hepatic venous flows once-through the in situ perfused rat liver to probe the abundance of drug metabolizing activities. Perihepatic venous O-deethylation activity for phenacetin and periportal sulfation activity for acetaminophen. *J. Pharmacol. Exp. Ther.* 247:690–700
81. El Mouelhi, M., Kauffman, F. C. 1986. Sublobular distribution of transferases and hydrolases associated with glucuronide, sulfate, and glutathione conjugation in human liver. *Hepatology* 6:450–56
82. Anundi, I. M., Kauffman, F. C., El-Mouelhi, M., Thurman, R. G. 1986. Hydrolysis of organic sulfates in periportal and pericentral regions of the liver lobule: Studies with 4-methylumbelliferyl sulfate in the perfused rat liver. *Mol. Pharmacol.* 29:599–605
83. Kashiwagi, T., Ji, S., Lemasters, J. J., Thurman, R. G. 1982. Rates of alcohol dehydrogenase-dependent ethanol metabolism in periportal and pericentral regions of the perfused rat liver. *Mol. Pharmacol.* 21:438–43
84. Pang, K. S., Terrell, J. A., Nelson, S. D., Feuer, K. F., Clements, M. J., Endrenyi, L. 1986. An enzyme-distributed system for lidocaine metabolism in the perfused rat liver preparation. *J. Pharmacokin. Biopharm.* 14:107–30
85. Pang, K. S., Cherry, W. F., Barker, F. III, Goresky, C. A. 1991. Esterases for enalapril hydrolysis is concentrated in the perihepatic venous region of the rat liver. *J. Pharmacol. Exp. Ther.* 257: 294–301
86. Goresky, C. A., Groom, A. C. 1984. Microcirculatory events in the liver and the spleen. In *Handbook of Physiology—The Cardiovascular System IV*, ed. E. M. Renkin, C. C. Michel, pp. 689–780. Washington, DC: Am. Physiol. Soc.
87. Goresky, C. A., Bach, G. G., Nadeau, E. 1975. Red cell carriage of label. Its limiting effect on the exchange of materials in the liver. *Cir. Res.* 36:328–51
88. Goresky, C. A., Schwab, A. J., Rose, C. P. 1988. Xenon handling in the liver: Red cell capacity effect. *Cir. Res.* 63:767–78
89. Pang, K. S., Barker, F. III, Schwab, A. J., Goresky, C. A. 1988. Red cell carriage of acetaminophen as studied by the technique of multiple indicator dilution in perfused rat liver. *Hepatology* 8:1384 (Abstr. 667)
90. Gillette, J. R. 1973. ●verview of drug-protein binding. *Proc. NY Acad. Sci.* 226:6–17
91. Weisiger, R. A. 1985. Dissociation from albumin: A potentially rate-limiting step in the clearance of substanccs. *Proc. Natl. Acad. Sci. USA* 82:1563–67
92. Levy, G., Yacobi, A. 1974. Effect of protein binding on elimination of warfarin. *J. Pharm. Sci.* 63:805–6
93. Grausz, H., Schmid, R. 1971. Reciprocal relation between plasma albumin level and hepatic sulfobromophthalein removal. *New Engl. J. Med.* 284:1403–4
94. Barnhart, J. R., Clarenburg, R. 1973. Factors determining the clearance of bilirubin in perfused rat liver. *Am. J. Physiol.* 225:497–508
95. Schary, W. L., Rowland, M. 1983. Protein binding and hepatic clearance: studies with tolbutamide, a drug of low intrinsic clearance, in the isolated perfused rat liver preparation. *J. Pharmacokin. Biopharm.* 11:225–43
96. Tsao, S. C., Sugiyama, Y., Sawada, Y., Nagase, S., Iga, T., Hanano, M. 1986. Effect of albumin on hepatic uptake of warfarin in normal and analbuminemic mutant rats: Analysis by multiple indicator dilution method. *J. Pharmacokin. Biopharm.* 14:51–65

97. Sorrentino, D., Robinson, R. B., Kiang, C-L., Berk, P. D. 1989. At physiological albumin/oleate concentrations oleate uptake by isolated hepatocytes, cardiac myocytes, and adipocytes is a saturable function of the unbound oleate concentration. Uptake kinetics are consistent with the conventional theory. *J. Clin. Invest.* 84:1325–33
98. Goresky, C. A., Pang, K. S., Schwab, A. J., Barker, F. III, Cherry, W. F., Bach, G. G. 1992. Protein binding effects in acetaminophen sulfate entry into perfused rat liver. *Hepatology* In press
99. St-Pierre, M. V., van den Berg, D., Pang, K. S. 1990. Physiological modeling of drug and metabolite: Disposition of oxazepam and oxazepam glucuronides in the recirculating, perfused rat liver preparation. *J. Pharmacokin. Biopharm.* 18:423–48
100. St-Pierre, M. V., Gasinska, I., Pang, K. S. 1992. Sequential elimination of oxazepam in the perfused mouse liver preparation. I. As metabolites of temazepam and nordiazepam. *J. Pharmacokin. Biopharm.* Submitted
101. St-Pierre, M. V., Pang, K. S. 1992. Sequential elimination of oxazepam in the perfused mouse liver preparation. II. As sequential metabolites of diazepam. *J. Pharmacokin. Biopharm.* Submitted
102. Morris, M. E., Yuen, V., Tang, B. K., Pang, K. S. 1988. Competing pathways in drug metabolism. I. Effect of varying input concentrations on gentisamide conjugation in the once-through in situ perfused rat liver preparation. *J. Pharmacol. Exp. Ther.* 245:614–52
103. Xu, X., Tang, B. K., Pang, K. S. 1990. Sequential metabolism of salicylamide exclusively to gentisamide-5-glucuronide and not gentisamide sulfate conjugates in the single pass in situ perfused rat liver. *J. Pharmacol. Exp. Ther.* 253:965–73
104. Pohl, L. R., Thomassen, D., Pumpford, N. R., Bulter, L. E., Satoh, H., et al. 1990. Hapten carrier conjugates associated with halothane hepatitis. *Adv. Exp. Med. Biol.* 283:111–20
105. Pang, K. S., Xu, X., Morris, M. E., Yuen, V. 1987. Kinetic modeling of conjugations in liver. *Fed. Proc.* 46: 2439–41
106. Morris, M. E., Pang, K. S. 1987. Competition between two enzymes for substrate removal in liver: Modulating effects of competitive pathways. *J. Pharmacokin. Biopharm.* 15:473–96
107. Pang, K. S., Koster, H., Halsema, I. C. M., Scholtens, E., Mulder, G. J. 1981. Aberrant pharmacokinetics of harmol in the perfused rat liver preparation: Sulfate and glucuronide conjugations. *J. Pharmacol. Exp. Ther.* 219:134–40
108. Koster, H., Halsema, I., Pang, K. S., Scholtens, E., Mulder, G. J. 1982. Kinetics of sulfation and glucuronidation of harmol in the perfused rat liver preparation. Disappearance of aberrancies in glucuronidation kinetics by inhibition of sulfation. *Biochem. Pharmacol.* 31: 3023–38
109. Pang, K. S. 1983. The effect of intercellular distribution of drug metabolizing enzymes on the kinetics of stable metabolite formation and elimination by liver: First-pass effects. *Drug Metab. Rev.* 14:61–76
110. Pang, K. S., Kong, P., Terrell, J. A., Billings, R. E. 1985. Metabolism of acetaminophen and phenacetin by isolated rat hepatocytes. A system in which the spatial organization inherent in the liver is disrupted. *Drug Metab. Dispos.* 13:42–50
111. Brauer, R. W., Leong, G. F., McElroy, R. F., Holloway, R. J. 1956. Circulatory pathways in the rat liver as revealed by P^{32} chromic phosphate colloid uptake in the perfused rat liver. *Am. J. Physiol.* 184:593–98
112. Whitsett, J. L., Dayton, P. G., McNay, T. L. 1971. The effect of hepatic blood flow on the hepatic removal rate of oxyphenbutazone in the dog. *J. Pharmacol. Exp. Ther.* 177:246–55
113. Keiding, E., Chiarantini, E. 1978. Effect of sinusoidal perfusion on galactose elimination kinetics in perfused rat liver. *J. Pharmacol. Exp. Ther.* 205: 465–70
114. Shand, D. G., Kornhauser, D. M., Wilkinson, G. R. 1975. Effects of route of administration and blood flow on hepatic elimination. *J. Pharmacol. Exp. Ther.* 195:424–32
115. Ahmad, A. B., Bennett, P. N., Rowland, M. 1983. Models of hepatic drug clearance: Discrimination between the"well-stirred" and "parallel-tube" models. *J. Pharm. Pharmacol.* 35:219–24
116. Dawson, J. R., Weitering, J. G., Mulder, G. J., Stillwell, R. N., Pang, K. S. 1985. Alteration of transit time and direction of flow to probe the heterogeneous distribution of conjugation activities for harmol in the perfused rat liver preparation. *J. Pharmacol. Exp. Ther.* 234:691–97
117. Pang, K. S., Rowland, M. 1977. Hepatic clearance of drugs. III. Additional experimental evidence for the accep-

tance of the "well-stirred" model using metabolite (MEGX) data generated from lidocaine. *J. Pharmacokin. Biopharm.* 5:681–90

118. Pang, K. S., Mulder, G. J. 1990. A Commentary: Effect of flow on formation of metabolites. *Drug Metab. Dispos.* 18:270–75

119a. Jusko W. J., Gretch, M. 1976. Plasma and tissue protein binding of drugs in pharmacokinetics. *Drug Metab. Rev.* 5:43–140

119b. Rowland, M. 1984. Protein binding and drug clearance. *Clin. Pharmacokin.* 9(Suppl.1):10–17

119c. Øie, S. 1986. Drug distribution and binding. *J. Clin. Pharmacol.* 26:583–86

119. Huang, J. D., Øie, S. 1984. Hepatic elimination of drugs with concentration-dependent serum protein binding. *J. Pharmacokin. Biopharm.* 12:67–81

120. Jansen, J. A. 1981. Influence of plasma protein binding kinetics on hepatic clearance assessed from a "tube" model and a "well-stirred" model. *J. Pharmacokin. Biopharm.* 19:15–26

121. Smallwood, R. H., Mihaly, G. W., Smallwood, R. A., Morgan, D. J. 1988. Effect of a protein binding change on unbound and total plasma concentrations for drugs of intermediate hepatic extraction. *J. Pharmacokin. Biopharm.* 16: 529–42

122. Rubin, G. M., Tozer, T. N. 1986. Hepatic binding and Michaelis-Menten metabolism of drugs. *J. Pharm. Sci.* 75:660–63

123. Wosilait, W. D., Garten, S. 1972. Computation of unbound anticoagulant values in plasma. *Res. Commun. Chem. Pathol. Pharmacol.* 3:285–91

124. Øie, S., Levy, G. 1975. Effect of plasma protein binding on elimination of bilirubin. *J. Pharm. Sci.* 64:1433–34

125. Gugler, R., Mueller, G. 1978. Plasma protein binding of valproic acid in healthy subjects and in patients with renal disease. *Br. J. Clin. Pharmacol.* 5:441–46

126. Xu, X., Pang, K. S. 1992. Nonlinear protein binding and heterogeneity of drug metabolizing enzyme on hepatic drug removal. *J. Pharmacokin. Biopharm.* Submitted

127. Silverman, M., Goresky, C. A. 1965. A unified kinetic hypothesis of carrier mediated transport and its applications. *Biophys. J.* 5:487–509

128. Goresky, C. A., Bach, G. G., Nadeau, B. E. 1973. On the uptake of materials by the intact liver: the transport and net removal of galactose. *J. Clin. Invest.* 52:991–1009

129. Goresky, C. A., Bach, G. G., Nadeau, B. E. 1973. Uptake of materials by the intact liver. The exchange of glucose across cell membranes. *J. Clin. Invest.* 53:634–46

130. Scharschmidt, B. F., Waggoner, J. G., Berk, P. D. 1975. Hepatic organic anion uptake in the rat ICG, BSP and bilirubin. *J. Clin. Invest.* 56:1280–92

131. Reichen, J., Paumgartner, G. 1975. Kinetics of taurocholate uptake by the perfused rat liver. *Gastroenterology* 68:132–36

132. Dietmaier, A., Gasser, R., Graf, J., Peterlik, M. 1976. Investigations on the sodium dependence of bile acid fluxes in the isolated perfused rat liver. *Biochim. Biophys. Acta* 443:81–91

133. Graf, J., Peterlik, M. 1976. Ouabain-mediated sodium uptake and bile formation by isolated perfused rat liver. *Am. J. Physiol.* 230:876–85

134. Reichen, J., Paumgartner, G. 1976. Uptake of bile acids by perfused rat liver. *Am. J. Physiol.* 231:734–42

135. Scharschmidt, B. F., Stephens, J. E. 1981. Transport of sodium, chloride, and taurocholate by cultured rat hepatocytes. *Proc. Natl. Acad. Sci. USA* 78: 986–90

136. Novak, D. N., Ryckman, F. C., Suchy, F. J. 1989. Taurocholate transport by basolateral plasma membrane vesicles isolated from human liver. *Hepatology* 10:447–53

137. Stremmel, W., Gerber, M. A., Glezerov, V., Thung, S. N., Kochwa, S., Berk, P. D. 1983. Physicochemical and immunohistological studies of a sulfobromophthalein- and bilirubin binding proteins from rat liver plasma membranes. *J. Clin. Invest.* 71:1796–805

138. Duffy, M. C., Blitzer, B. L., Boyer, J. L. 1983. Direct determination of the driving forces for taurocholate uptake into rat liver plasma membrane vesicles. *J. Clin. Invest.* 72:1470–81

139. Potter, B. J., Blades, F., Shepard, M. D., Thung, S. M., Burke, P. D. 1987. The kinetics of sulfobromophthalein uptake by rat liver sinusoidal vesicles. *Biochim. Biophys. Acta* 898:159–71

140. Wolkoff, A. W., Samuelson, A. C., Johansen, K. L., Nakata, R., Withers, D. M., Sosiak. A. 1987. Influence of Cl^- on organic anion trnsport in short-term cultured rat hepatocytes and isolated perfused rat liver. *J. Clin. Invest.* 79:1259–68

141. Miccio, M., Baldini, G., Basso, V., Gazzin, B., Lunazzi, G. C., et al. 1989. Bilitranslocase is the protein responsible for the elctrogenic movement of sulfo-

bromophthalein in plasma membrane vesicles from rat liver: immunochemical evidence using mono and poly-clonal antibodies. *Biochim. Biophys. Acta* 981: 115–20

142. Iwamoto, K., Eaton, D. L., Klaassen, C. D. 1983. Uptake of morphine and nalorphine by isolated hepatocytes. *J. Pharmacol. Exp. Ther.* 206:181–89
143. Ishii, E. L., Schwab, A. J., Bracht, A. 1987. Inhibition of monosaccharide transport in the intact rat liver by stevioside. *Biochem. Pharmacol.* 36:1417–33
144. Sato, H., Sugiyama, Y., Miyauchi, S., Sawada, Y., Iga, T., Hanano, M. 1986. A simulation study on the effect of a uniform diffusional barrier across hepatocytes on drug metabolism by evenly or unevenly distributed uni-enzyme in the liver. *J. Pharm. Sci.* 75:3–8
145. Bartoli, G., Sies, H. 1978. Reduced and oxidized glutathione efflux from liver. *FEBS Lett.* 86:89–91
146. Dedrick, R. L., Zaharko, D. S., Lutz, R. J. 1973. Transport and binding of methotrexate in vivo. *J. Pharm. Sci.* 62:882–90
147. Lutz, R. L., Galbraith, W. B., Dedrick, R. L., Schrager, R., Mellett, L. B. 1977. A model for the kinetics of distribution of actinomycin-D in the beagle dog. *J. Pharmacol. Exp. Ther.* 200:469–78
148. Chen, C. N., Coleman, D. L., Andrade, J. D., Temple, A. R. 1978. Pharmacokinetic model for salicylate in cerebrospinal fluid, blood, organs, and tissues. *J. Pharm. Sci.* 67:38–45
149. Miyauchi, S., Sugiyama, Y., Sawada, Y., Iga, T., Hanano, M. 1987. Conjugative metabolism of 4-methylumbelliferone in the rat liver: verification of the sequestration process in multiple indicator dilution experiments. *Chem. Pharm. Bull.* 35:4241–48
150. Miyauchi, S., Sugiyama, Y., Iga, T., Hanano, M. 1988. Conjugative metabolism of 4-methylumbelliferone in rats. *J. Pharm. Sci.* 77:688–92
151. Steele, J. W., Yagen, B., Hernandez, O., Cox, R. H., Smith, B. R., Bend, J. R. 1981. The metabolism and excretion of styrene oxide-glutathione conjugates in the rat and by isolated perfused liver, lung, and kidney preparations. *J. Pharmacol. Exp. Ther.* 219:35–41
152. de Lannoy, I. A. M., Pang, K. S. 1986. A commentary. The presence of diffusional barriers on drug and metabolite kinetics. Enalaprilat as a generated versus preformed metabolite. *Drug Metab. Dispos.* 14:513–20
153. de Lannoy, I. A. M., Pang, K. S. 1987. Diffusional barriers on drug and metabolite kinetics. *Drug Metab. Dispos.* 15: 51–58
154. Schwab, A. J., Barker, F. III, Goresky, C. A., Pang, K. S. 1990. Transfer of enalaprilat across rat liver cell membranes is barrier-limited. *Am. J. Physiol.* 258:G461–75
155. Pang, K. S., Cherry, W. F., Terrell, J. A., Ulm, E. H. 1984. Disposition of enalapril and its diacid metabolite, enalaprilat, in a perfused rat liver preparation. Presence of a diffusional barrier for enalaprilat into hepatocytes. *Drug Metab. Dispos.* 12:309–13
156. de Lannoy, I. A. M., Pang, K. S. 1992. Combined recirculation of the rat liver and kidney: Studies with enalapril and enalaprilat. *J. Pharmacokin. Biopharm.* Submitted
157. de Lannoy, I. A. M., Nespeca, R., Pang, K. S. 1989. Renal handling of enalapril and its metabolite, enalaprilat, in the isolated red blood cell-perfused rat kidney. *J. Pharmacol. Exp. Ther.* 251:1211–22
158. Gibaldi, M., Boyes, R. N., Feldman, S. 1971. Influence of first-pass effect on availability of drugs on oral administration. *J. Pharm. Sci.* 60:1338–40
159. Pang, K. S., Gillette, J. R. 1978. Theoretical examination of the effects of gut wall metabolism, hepatic elimination, and enterohepatic recycling upon estimates of bioavailability and of hepatic blood flow. *J. Pharmacokin. Biopharm.* 6:355–65
160. Cassidy, M. K., Houston, J. B. 1980. In vivo assessment of extrahepatic conjugative metabolism in first pass effects using the model compound phenol. *J. Pharm. Pharmacol.* 32:57–59
161. Mulder, G. J., Weitering, G. J., Scholtens, E., Dawson, J. R., Pang, K. S. 1984. Extrahepatic sulfation and glucuronidation in the rat. Determinations of the hepatic extraction ratio of harmol and the extrahepatic contribution to harmol conjugation. *Biochem. Pharmacol.* 33:3081–87
162. Pang, K. S. 1986. Metabolic first-pass effect. *J. Clin. Pharmacol.* 26:580–82
163. Mulder, G. J., Brouwer, S., Weitering, J. G., Scholtens, E., Pang, K. S. 1985. Glucuronidation and sulfation in the rat in vivo: The role of the liver and the intestine in the in vivo clearance of 4-methyl-umbelliferone. *Biochem. Pharmacol.* 34:1325–29
164. Hirayama, H., Morgado, J., Gasinska, I., Pang, K. S. 1990. Estimations of intestinal and liver extraction in the in vivo rat: studies on gentisamide conjugation. *Drug Metab. Dispos.* 18:580–87

165. Pang, K. S., Cherry, W. F., Ulm, E. H. 1985. Disposition of enalapril in the intestine-liver preparation: Absorption, metabolism, and first-pass effects. *J. Pharmacol. Exp. Ther.* 233:788–95
166. Pang, K. S., Fayz, S., Yuen, V., te Koppele, J., Mulder, G. J. 1986. Absorption and metabolism of acetaminophen by the in situ perfused rat intestine preparation. *Drug Metab. Dispos.* 14:102–13
167. Hirayama, H., Xu, X., Pang, K. S. 1989. Viability of the recirculating perfused rat intestine and intestine-liver preparations. *Am. J. Physiol.* 257:G249–58
168. Xu, X., Hirayama, H., Pang, K. S. 1989. First-pass metabolism of salicylamide: Studies in the once-through vascularly perfused rat intestine-liver preparation. *Drug Metab. Dispos.* 17:556–63
169. Hirayama, H., Pang, K. S. 1990. First-pass metabolism of gentisamide: Influence of intestinal metabolism on hepatic formation of conjugates. Studies in the once-through vascularly perfused rat intestine-liver preparation. *Drug Metab. Dispos.* 18:588–94
170. Zimmerman, C., Ratna, S., LeBoeuf, E., Pang, K. S. 1991. A high pressure liquid chromatographic assay for 4-methylumbelliferone and its conjugates. *J. Chromatogr.* 563:83–94